REPORT DOCUMENTATION PAGE

Form Approved
OMB No. 0704-0188

1. REPORT DATE *(DD-MM-YYYY)*	2. REPORT TYPE	3. DATES COVERED *(From - To)*
11-05-2010		

4. TITLE AND SUBTITLE
Convective Heat Transfer Enhancement Using Alternating Magnetic Fields and Particle Laden Fluid Applied to the Microscale

5a. CONTRACT NUMBER

5b. GRANT NUMBER

5c. PROGRAM ELEMENT NUMBER

6. AUTHOR(S)
Golden, James Hollis

5d. PROJECT NUMBER

5e. TASK NUMBER

5f. WORK UNIT NUMBER

7. PERFORMING ORGANIZATION NAME(S) AND ADDRESS(ES)

8. PERFORMING ORGANIZATION REPORT NUMBER

9. SPONSORING/MONITORING AGENCY NAME(S) AND ADDRESS(ES)
U.S. Naval Academy
Annapolis, MD 21402

10. SPONSOR/MONITOR'S ACRONYM(S)

11. SPONSOR/MONITOR'S REPORT NUMBER(S)
Trident Scholar Report no. 389 (2010)

12. DISTRIBUTION/AVAILABILITY STATEMENT
This document has been approved for public release; its distribution is UNLIMITED

13. SUPPLEMENTARY NOTES

14. ABSTRACT

This research investigated the miniaturization of a novel heat transfer enhancement technique. The technique, using alternating magnetic fields to influence a ferromagnetic particle laden fluid, was demonstrated to be effective on conventional scales using an oil based suspension, increasing the coefficient of heat transfer, h, by 260%. In order to determine the viability of this enhancement technique at smaller scales using a water based suspension, an experimental apparatus was designed to measure the coefficient of convective heat transfer in mini- and micro-scale flows. Water based suspensions of ferromagnetic particles were pumped through a 1.1 mm diameter heated tube. External alternating magnetic fields acted on the suspension, causing the particles to be attracted to and then released from the heat transfer surface. The efficacy of this enhancement technique was determined by comparing the heat transfer coefficients between enhanced and non-enhanced trials, while also considering the resulting increase in pressure loss. Dispersions of Fe and Fe3O4 particles were used during experimentation.

15. SUBJECT TERMS
Heat Transfer, Ferromagnetic Fluid, Microscale

16. SECURITY CLASSIFICATION OF:			17. LIMITATION OF ABSTRACT	18. NUMBER OF PAGES	19a. NAME OF RESPONSIBLE PERSON
a. REPORT	b. ABSTRACT	c. THIS PAGE		49	19b. TELEPHONE NUMBER *(Include area code)*

U.S.N.A. --- Trident Scholar project report; no. 389 (2010)

Convective Heat Transfer Enhancement Using Alternating Magnetic Fields and Particle Laden Fluid Applied to the Microscale

by

Midshipman 1/c James H. Golden
United States Naval Academy
Annapolis, Maryland

_____
(signature)

Certification of Advisers Approval

Associate Professor Mark M. Murray
Mechanical Engineering Department

_____
(signature)

_____
(date)

Associate Professor Andrew N. Smith
Mechanical Engineering Department

_____
(signature)

_____
(date)

Acceptance for the Trident Scholar Committee

Professor Carl E. Wick
Associate Director of Midshipman Research

_____
(signature)

_____
(date)

USNA-1531-2

Abstract

Increasing demands for heat removal necessitate the development of more effective thermal management technologies. In applications employing convective heat transfer, one direction of innovation is miniaturization, which affords increased rates of heat transfer. This research investigated the miniaturization of a novel heat transfer enhancement technique. The technique, using alternating magnetic fields to influence a ferromagnetic particle laden fluid, was demonstrated to be effective on conventional scales using an oil based suspension, increasing the coefficient of heat transfer, *h*, by 260%. In order to determine the viability of this enhancement technique at smaller scales using a water based suspension, an experimental apparatus was designed to measure the coefficient of convective heat transfer in mini- and micro-scale flows. Water based suspensions of ferromagnetic particles were pumped through a 1.1 mm diameter heated tube. External alternating magnetic fields acted on the suspension, causing the particles to be attracted to and then released from the heat transfer surface. It was anticipated that the modification of the flow regime would enhance heat transfer by disrupting the laminar flow conditions, and that the particles would serve to increase the heat transfer surface area. This flow modification was also expected to increase the differential pressure across the test section. The efficacy of this enhancement technique was determined by comparing the heat transfer coefficients between enhanced and non-enhanced trials, while also considering the resulting increase in pressure loss. Dispersions of Fe and Fe_3O_4 particles were used during experimentation. When testing the Fe_3O_4 suspension an 86% increase in *h* was observed, although localized heat transfer modification persisted after the removal of the magnetic fields, likely due to particle aggregation in the test section. Trials employing the Fe suspension resulted in a flow modification similar to the conventional experiment and a 23% increase in the measured convective heat transfer coefficient.

Keywords

Convection, Heat Transfer Enhancement, Particle-Laden Fluid, Magnetic Fluid

Acknowledgements

The author would like to acknowledge the efforts of the Trident Advisors, Dr. Mark Murray and Dr. Andrew Smith, who have not only provided academic guidance and direction throughout the successes and frustrations of this research, but have served as professional and personal mentors. They have instructed the principles of effective and thorough research, to which persistence through frustration is central.

The author would also like to acknowledge the sound advise and salient example of his brother, 2nd Lieutenant Daniel Golden, USMC, a Naval Academy graduate and Trident Scholar from the Class of 2008.

Table of Contents

List of Tables

List of Figures

List of Symbols

Micron or micrometer	$1x10^{-6}$ m
Nanometer	$1x10^{-9}$ m
h	Coefficient of Convective Heat Transfer
T(F)	Tube Surface Temperature, Fahrenheit
L	Luminance
q_{conv}	Heat Transferred By Convection
m_{dot}	Mass Flowrate of Fluid
C_p	Specific Heat of Fluid
$T_{fluid,O}$	Fluid Inlet Temperature
$T_{fluid,I}$	Fluid Exit Temperature
dq_{conv}	Heat Transferred into Differential Control Volume
dT_{fluid}	Change in Fluid Temperature Across Differential Control Volume
q_s"	Surface Heat Flux
P	Perimeter
D	Hydraulic Diameter
dx	Length of Differential Control Volume
$T_{fluid}(x)$	Fluid Temperature at Position x
$h_{conv}(x)$	Coefficient of Convective Heat Transfer at Position x
Fe	Iron
Fe_3O_4	Iron(II,III)Oxide, Magnetite

1. Introduction

1.1
Motivation

Thermal management is a central design consideration for many engineering technologies, from the complex to the commonplace. Many applications, like thermal power systems, rely on effective heat transfer to extract the maximum work from a given fuel source. Other systems employ thermal management principles to efficiently remove waste heat, which would otherwise degrade their operation. One specific example is in the design of electronic components, whose silicon-based microprocessors often lose their functionality above critical temperatures. In many systems, like the commonplace CPU, waste heat is effectively removed through a simple air-cooled heat sink. However, as electronics components become smaller, faster and more powerful, they are requiring more effective heat removal, pushing the limits of traditional thermal management practices. Seeking to improve the effectiveness of conventional thermal management techniques to satisfy the demand for high heat flux removal, thermal engineers have recently focused on the development of heat transfer enhancement techniques.

1.2
Background: Convective Heat Transfer Enhancement

In many thermal management applications, convective heat transfer is the principle means of conveying energy from one body to another. Convective heat transfer refers to the exchange of energy from a solid surface to a moving fluid. This fluid flow can be driven externally by a fan or pump, termed forced convection, or can be induced by a temperature dependent density gradient, termed natural convection. Convection can also be classified according to the phase of the fluid; single phase applications do not change phase, while multi phase applications take advantage of the latent heat of transformation. This research is concerned with heat transfer enhancement in single phased forced convection.

Heat transfer in single phased forced convection applications can be envisioned as two separate processes: the conduction of heat from the solid surface to the fluid and the conveyance of energy away from the surface with the mass flow of the fluid. The rate of conduction is governed by both the thermal conductivity of the fluid and the flow conditions near the surface. Flow conditions that do not allow for fluid near the solid surface to be replaced by fluid from the bulk flow inhibit effective heat transfer. The rate of the conveyance of energy away from the heat transfer surface is influenced by both the heat capacity and viscosity of the fluid, in addition to the mass flow rate of the flow. Convective heat transfer enhancements are realized by optimizing flow conditions and selecting a fluid with an optimal combination of thermophysical properties including thermal conductivity, density, specific heat capacity, and viscosity.[1]

Engineers have long sought to increase the effectiveness of convective heat transfer in thermal management devices, and their enhancement techniques are classified in two categories, passive and active. Passive enhancement techniques typically refer to permanent modifications that do not require the addition of external energy. For example, passive techniques may involve increasing the heat transfer surface's roughness or inserting flow disruptors into the tube. Active enhancement techniques refer to a continuous external effort to improve heat transfer that typically requires external energy input. Active techniques include measures to manipulate the flow through the application of vibrations or electrostatic forces and techniques employing flow pulsation and variable surface roughness. All of these enhancement techniques increase heat transfer by tripping the flow from a laminar to a turbulent flow regime, creating a component of the flow normal to the surface or by disrupting the viscous sublayer of turbulent flow. Turbulent flow is generally advantageous because the turbulent flow regime is marked by chaotic mixing of the flow, bringing more of the fluid in contact with the heat transfer surface and increasing the rate of heat transfer.[2]

One recent, novel passive enhancement technique realizes heat transfer enhancement by increasing the thermal conductivity of the fluid through the addition of particles to the fluid. While the thermal performance of particle-laden flows has been well studied, [3-4] researchers have created a new type of particle-laden fluid using nanoparticels that have anomalously increased

the thermal conductivity of the base fluid.[5] Suspensions created from these nanometer sized particles, termed nanofluids, have been shown to significantly increase heat transfer rates, even when at small concentrations.[6-7] Additionally because of the small particle size, nanofluids are not limited by the rheological and stability problems that preclude the widespread use of conventional particle-laden fluids.[8] However, nanofluid performance is not consistently established in the literature, with some investigations showing less heat transfer enhancement than expected.[9]

Seeking further enhancement to convective heat transfer, researchers have been drawn to the high heat flux potentials of microfluidic devices. Microchannel flows, with hydraulic diameter between 200 and 10 micrometers, represent a particularly promising advance in thermal management, because heat transfer coefficients are inversely proportional to hydraulic diameter.[10] Microchannels may provide smaller and more localized thermal management solutions for high heat flux removal in applications ranging from microprocessor cooling to compact fuel cell operation. While single phase convective heat transfer enhancement schemes are well established and documented for conventional sized flows (greater than 3mm), the applicability of these enhancement methods to minichannel (3mm to 200 microns) and microchannel (200 to 10 microns) flows is the subject of ongoing research.[11] This research focuses on the application of a novel heat transfer enhancement technique proven on the conventional scale to the mini and microchannel scales.

1.3
Background: Conventional Scale Enhancement Technique [12]

The fundamental concept of this heat transfer enhancement scheme is to intelligently combine the superior thermal conductivity characteristics of certain solids with the low viscosity and high heat capacity of appropriate fluids to enhance the overall heat transfer characteristics of a heat exchanger. The heat transfer medium consists of highly conductive ferromagnetic particles suspended in a base fluid. A time varying magnetic field is used to manipulate the flow regime, as visualized in Figure 1.1. An activated magnetic field attracts and holds the particles to the

wall. The magnetic field is deactivated and the particles are released back into the fluid. An opposing electromagnet on the opposite channel wall, out of phase with the first, provides the motive force for the particle release and promotes flow normal to the heat transfer surface.

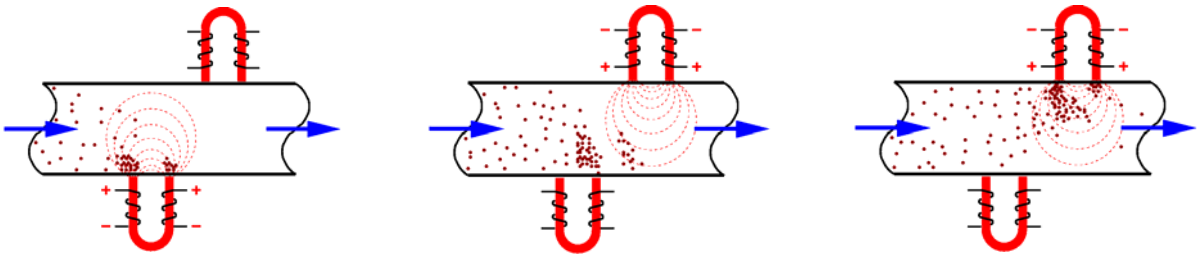

Particles attracted to lower electromagnet while energized.

Particles released from lower electromagnet into bulk fluid and start of attraction toward energized upper electromagnet.

Particles attracted to upper electromagnet while energized.

Figure 1.1: Diagrams of magnetic particles being attracted to and then released by the magnetic fields of energized electromagnets

The manipulation of the particle-laden fluid is expected to provide heat transfer enhancement through three distinct processes. First, the particles, with greater thermal conductivity than the base fluid, quickly conduct heat from the wall when the magnetic field is activated. After the particles are released from the wall, they enter the bulk fluid flow; the particles, surrounded in the bulk fluid, serve to increase the overall heat transfer surface area. In addition to this thermal phenomenon, the enhancement technique modifies the flow conditions in two ways. First, the attraction and repulsion of the particles initiates flow perpendicular to the bulk flow and normal to the channel wall, bringing more of the bulk fluid in contact with the heat transfer surface and disrupting the laminar flow regime. Additionally, when the particles are magnetically attracted to the channel wall, they temporarily aggregate into geometries resembling the fins traditionally used to enhance heat transfer. These particle formations serve to disrupt the laminar flow condition and increase the flow's vorticity.

Collectively, these phenomena were shown to significantly increase the rate of heat transfer in previous conventional scaled experiments. The conventional scale investigation employed a working fluid of 5% (by weight) 300 micron iron filings dispersed in mineral oil. The working fluid passed through a 1.38 cm heated tube. The temperature of the fluid and the tube surface was measured using thermocouples and an infrared camera, and the fluid's heat transfer coefficient was calculated from this data. The experiment was conducted under enhanced and non-enhanced conditions. At maximum enhancement, which occurred at a magnet switching frequency of 2 Hz, the heat transfer coefficient increased by 267% from 57 to 205 W/m^2K while differential pressure was increased by 48% over the non-enhanced trials. This increased heat transfer efficiency is visualized in Figure 1.2, which shows a significantly cooler tube surface temperature when utilizing the enhancement technique.

The conventional scale investigation into this novel heat transfer enhancement technique produced impressive results; however, its real application demands a smaller scale. Miniaturization of this enhancement technique represents a promising advance in thermal management technology, and is a contribution to the active field of microscale heat transfer.

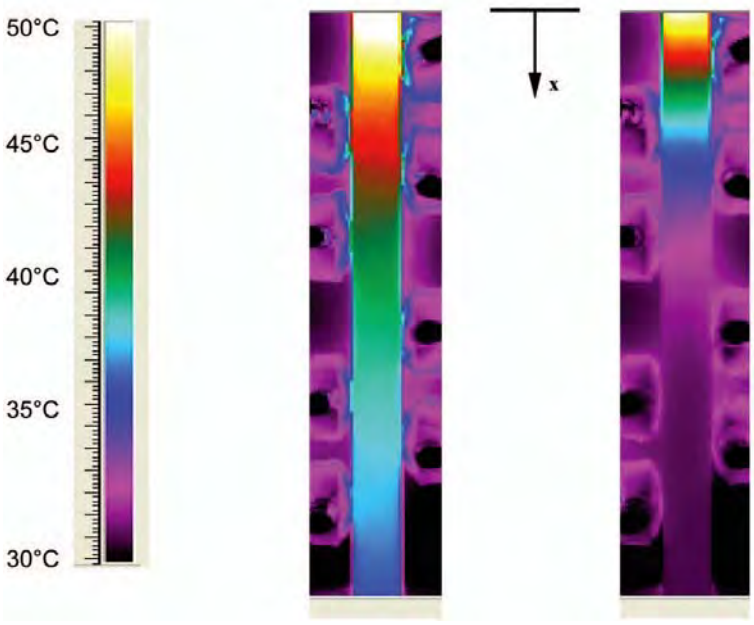

Figure 1.2: IR camera images of test section without enhancement, left, and with magnetic enhancement, right

2. Experimental Apparatus

2.1
Overview

In order to determine the efficacy of this novel heat transfer enhancement technique on smaller scales, an experimental apparatus capable of measuring the coefficient of convective heat transfer in mini- and micro-channel tubing was designed, fabricated and validated. Using this experimental apparatus, the surface temperature of a stainless steel test section heated under conditions of uniform surface heat flux was determined through infrared thermograph. The tube temperature, in addition to the inlet and outlet fluid temperatures, was used to calculate the coefficient of convective heat transfer for the flow. This aspect of the apparatus is similar to the experimental setup used by researchers at Stanford investigating the performance of nanofluids in microchannels.[13] The experimental apparatus also consisted of components necessary for the evaluation of the enhancement technique, including the electromagnet array and the particle-laden fluid system.

2.2
Component: Test Section

The enhancement technique under investigation at the mini- and micro-channel scales had been previously demonstrated on the conventional scale in 1.38 cm hydraulic diameter copper tubing. Miniaturized test sections, shown in Figure 2.1, were fabricated from tubing of three different hydraulic diameters, 1100, 250 and 100 microns, spanning the transition between the mini- and micro-channel flow regions. The test sections were prepared by soldering a header of 1/8” diameter stainless steel tubing to the ends of the micron-sized tubes. Silver solder was used for this connection, which effectively seals the junction to the micron-size tube and provides an electrical connection between the header and the test section. The test sections were uniformly

heated by passing a DC current through the tubing, heating the tube with a constant heat flux through resistance heating.

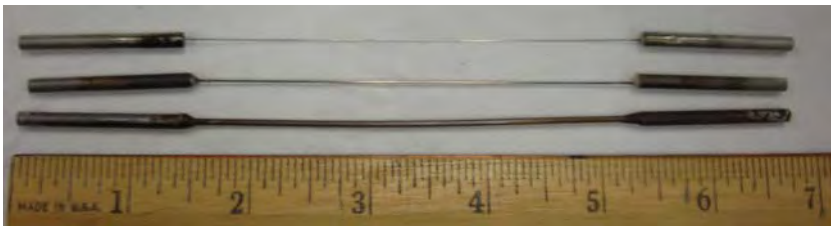

Figure 2.1: Image of 100, top, 250 and 1100, bottom, Micron Diameter Test Sections

A test section mount fabricated from PVC holds the tubing assembly during testing. The mount provides a stable foundation for the test section and electromagnet array, and is attached to a translating stage that facilitates the use of the high power, small field of view infrared camera lens. Initially the mount was fabricated from aluminum, but the large thermal mass of this metal mount served to sink heat from the test section, introducing an error into the experimental results. Constructing the mount from PVC mitigated this problem while still providing the necessary stable foundation, and is discussed in section 3.3. Figure 2.2 presents the Solidworks model of the test section mount and shows the design of the initial electromagnet array.

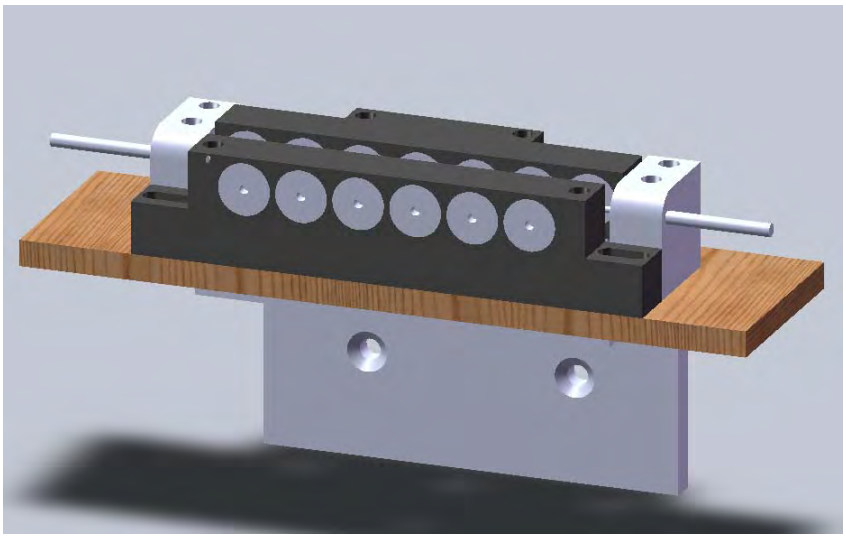

Figure 2.2: Solidworks Model of Initial Test Section Mount Design

2.3

Component: Data Acquisition System

In order to calculate the coefficient of convective heat transfer in the test section, several properties were collected during experimentation through a data acquisition system, including test section surface temperature, fluid temperatures at the inlet and outlet of the test section, differential pressure and flowrate.

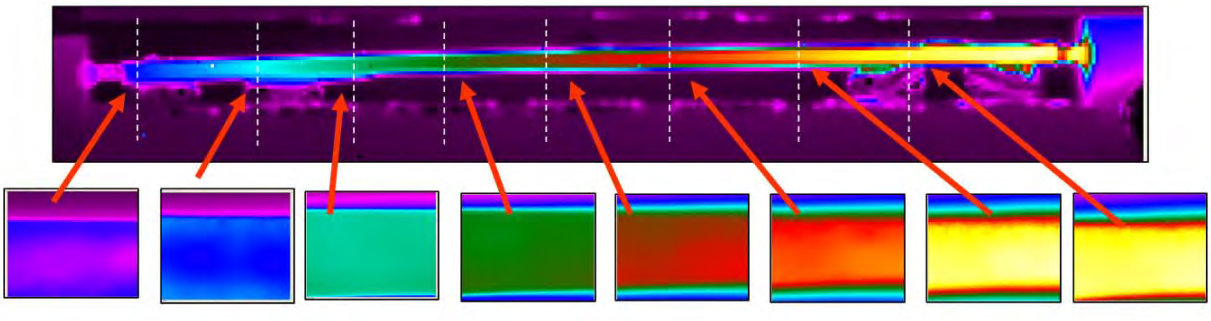

Figure 2.3: IR Images Demonstrating Continuous and Discrete Tube Temperature Measurement

An Indigo Systems infrared camera was used to determine the surface temperature of the test section. A standard lens was used during experimentation in the largest diameter test section, while a high power lens was intended to be used to focus in on the smaller tubing. In order to capture the temperature of the tubing across its entire length when using the high power lens, the test section was moved incrementally in front of the camera along a computer controlled translating stage. Examining the images taken at every increment and comparing the resulting tube temperature profile to one derived from a single, wide angle image confirmed the ability to determine the temperature along the length of the test section by sampling at discrete intervals. Figure 2.3 shows representative continuous and discrete tube surface imaging, and Figure 2.4 presents the tube temperature profiles derived from these images.

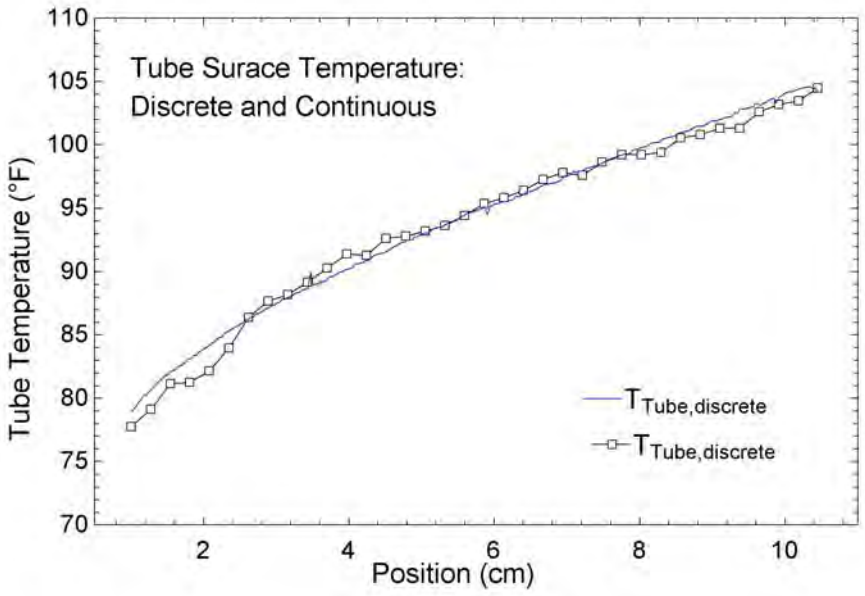

Figure 2.4: Tube Surface Temperature Profiles Taken from Discrete and Continuous IR Images

The infrared camera was calibrated before experimentation using an Electro Optical Industries blackbody simulator. This piece of precision equipment accurately emits radiation equivalent to a requested temperature. With the camera set to display the observed temperature in units of luminance, a third order transfer function converting luminance to temperature, presented below as Equation [1], was derived by taking data points from the blackbody simulator across the range of temperatures expected during experimentation, where T(F) is the Fahrenheit tube temperature and L is the observed luminance.

$$T\left(^{\circ}F\right) = 5.69\text{x}10^{-09}(L)^3 - 4.73\text{x}10^{-05}(L)^2 + 0.162\ (L) - 97.2 \qquad [1]$$

Other components of the data acquisition system were use to measure fluid properties during experimentation. Thermocouples in the flow immediately before and after the test section are used to determine the inlet and outlet fluid temperatures. Another thermocouple was used to document the ambient air temperature. These type K, thin wire thermocouples were calibrated before experimentation with both a boiling water bath and ice water slurry. Additionally, a differential pressure transducer (Omega PX26-001DV) was used to determine the pressure drop

across the test section. This transducer was calibrated to known pressures from a water column. These components of the data acquisition system were integrated into a LabVIEW virtual instrument through a National Instruments interface.

A high speed digital camera (Olympus i-Speed) was also utilized as an analysis tool to visually diagnose the efficacy of the enhancement technique. The camera was used in conjunction with a 1400 micron transparent glass tube to help determine the flow modification resulting from the external magnetic fields.

2.4
Component: Pumping System

A consistent pumping system capable of operating at the flowrates and pressures required for experimentation at such small scales was central to the experimental apparatus. Additionally, the nature of the particle-laden fluid influenced the design of the pumping system; the potential for sedimentation and aggregation of the suspended particles limited the types of practical pumps. Initial experimentation was conducted on an open circuit using a syringe pump in an experimental apparatus similar to that used by researchers at Stanford investigating nanofluid performance in microchannels.[14] In this open circuit configuration, the fluid is pumped from a syringe, through the test section, and into a reservoir. The apparatus was configured to facilitate recharging the syringe without introducing air into the system, eliminating the need to constantly purge the flow path. The syringe pump used a linear stepper motor to apply a constant rate of displacement to the syringe, enabling precise flowrate control. The maximum flowrate and pressure attainable using this pumping system is dependent on the syringe diameter; smaller syringes would be used during experimentation on the smaller tubing, which required a larger pressure. Figure 2.5 presents a picture of the syringe pump and Figure 2.6 presents a diagram of the open circuit system employed.

Figure 2.5: Image of Syringe Pump

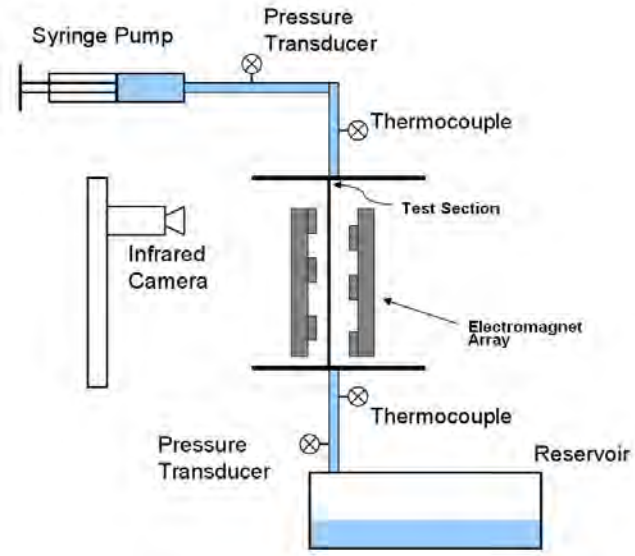

Figure 2.6: Diagram of Open Circuit System

During experimentation using the syringe pump, a noticeable change in the concentration of the fluid exiting the test section was observed. This inconsistency in the particle-laden fluid's concentration was likely due to sedimentation in the syringe. One measure taken to increase the consistency of the concentration of the heat transfer fluid was the implementation of a closed loop pumping system. A closed loop system using a suspension of iron filings in oil was employed in the successful conventional scale trials previously conducted,[15] and likely reduced the significance of particle settling. During latter experimental trials, the apparatus was reconfigured to employ an iron-based suspension using a peristaltic pump in a closed loop, more closely resembling the apparatus used during conventional scale trials. To remove the heat added to the fluid through the test section, a heat exchanger was incorporated into the closed loop.

Because this peristaltic pump's minimum flowrate was an order of magnitude higher than the flowrates used during experimentation on the open circuit system, bypasses were incorporated parallel to the test section. The parallel flow allowed for reasonable flow velocities in the test section, while maintaining high flow velocities in the rest of the loop. High flow velocities in the loop, above the critical settling velocity for the particles, are required to keep the particles in suspension. Figure 2.7 presents a diagram of the closed loop flow setup.

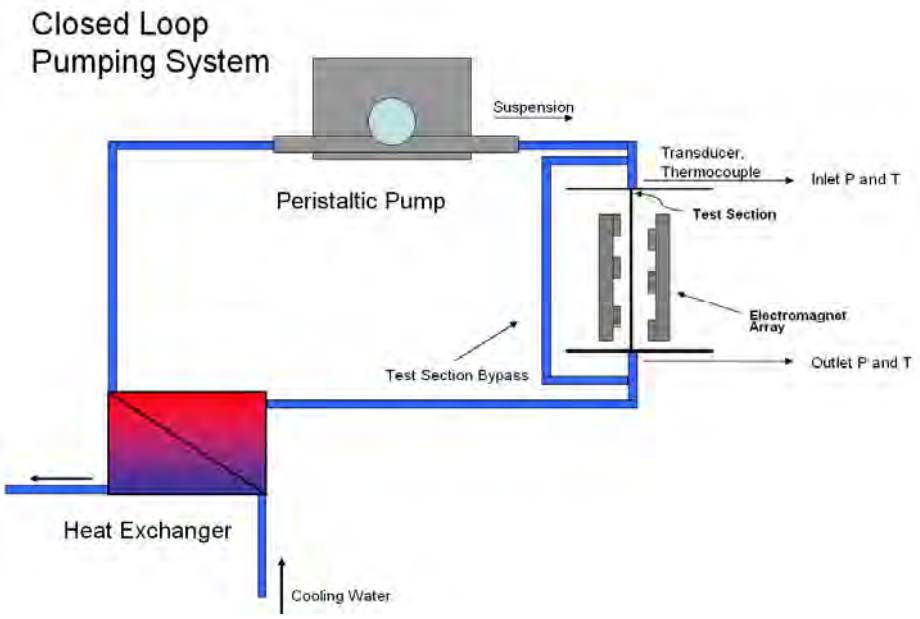

Figure 2.7: Diagram of Closed Loop Pumping System

2.5 *Component: Heat Transfer Fluid*

The particle-laden fluid used in this experimental apparatus is the central component of this enhancement technique, and its stability is a fundamental aspect of the effectiveness of the technique. For the enhancement technique to work as intended, the particles must come out of suspension and be attracted to the tube wall when acted on by the electromagnets. However, the particles must detach from the tube wall when released by the magnetic field and re-disperse into the bulk flow. Additionally, when the fluid is not in the test section, it must remain stable in order to prevent the clogging of the flow passages and to ensure a consistent particle concentration.

Fluid stability was not as critical an issue in the conventional scale experimentation, which used relatively large size iron filings (300 micron diameter) suspended in mineral oil. The large viscosity of the base fluid combined with large flow velocities in the closed loop system served to reduce the effect of sedimentation. However, because of the superior thermal performance of water over mineral oil, this current experiment was designed specifically to employ water-based heat transfer fluids. It was anticipated that significantly smaller particles would be required to form stable suspensions in water

The development of modern manufacturing processes and techniques has enabled the creation of nanometer sized particles. Homogeneous suspensions of these particles, termed nanofluids, have received a great deal of attention in the literature because of their supposedly anomalous thermal conductivity characteristics[16]. Many of these nanofluids are prepared using a chemical co-precipitation method, in which the small particles are chemically created while immersed in the base fluid. Another frequently used manufacturing process relies on physical methods to create and disperse the particles[17]. This physical approach is the method used to prepare the particle-laden fluid for this experimentation.

In this experiment, particle-laden fluids based on two different metallic particles were prepared. A 50 nanometer diameter powder of iron(II,III)oxide, known by its mineral name magnetite, was initially used during experimentation. Additionally, iron powder of 6-8 micron diameter was also used to prepare particle-laden fluids. When preparing the fluid, the powder was dispersed in deionized water through sonication, whereby high frequency acoustic energy breaks apart particle aggregates.[18] Sonication was conducted using both an ultrasonic bath and a much higher power probe sonicator. In fluid systems of both particles, sonication had the effect of temporarily forming a stable, homogeneous suspension. The duration of this stability was dependent on the size of the suspended particle and the method and length of sonication. Another method to aid in particle suspension is the addition of a surfactant. The surfactant sodium polyacrylate indefinitely prevented sedimentation in the magnetite fluid system. The surfactant acts by coating the particles and effectively changing the characteristics of their surface chemistry, reducing the attractive forces between particles; however, this effect is particular to the surfactant and the particle[19]. The surfactant used in the magnetite system was chosen based on its

stabilizing properties for iron oxide systems, as reported in the literature.[20] Sodium polyacrylate does not have the same stabilizing effect on the iron fluid system.

Both the iron and magnetite fluid systems displayed the strong attraction anticipated when subjected to magnetic fields, however, this attraction was significantly more pronounced in the iron system. Additionally, when the magnetic field was removed in these demonstrations, the iron particles quickly fell away, while the magnetite particles tended to aggregate. This contrast in behavior was explored during experimentation and would affect both fluid systems' performance in the experimental trials.

2.6

Component: Electromagnet Array

An array of electromagnets provides the manipulative force acting on the particle-laden fluid. In the final electromagnet array design, rows of 3 and 4 electromagnets (APW Company EM075-6-222) were mounted offset on the top and bottom of the test section, respectively. These magnets have a rated maximum power of 1.7 W, and produce a magnetic field with strength proportional to the applied current. During experimentation, the magnet arrays were operated at power levels in increments of their rated power. Table 1 presents the measured field strength for a single magnet at the power levels used during experimentation.

Table 1			
Electromagnet Performance		Magnet Resistance	21 Ohm
	Field Strength (Gauss)	Applied Current (Amp)	Applied Power (Watt)
1x Rated Power	55.57	0.28	1.65
2x Rated Power	111.14	0.39	3.29
3x Rated Power	166.71	0.49	4.94

Table 1: Electromagnet Performance at Various Power Levels

This maximum applied power is ultimately limited by resistive heating of the electromagnets, but even when operating at reasonable power levels, the electromagnets dissipated a significant and

influential amount of heat. Because this excess heat influenced the temperature of the test section, adding a potential source of experimental error, the mount was redesigned to actively cool the magnets using a recirculating chiller. Mounting screws into the magnet cores and a coating of thermal grease strengthened the thermal connection between the magnets and the cooled array. The effect of magnet heating on the performance of the experimental apparatus, which motivated its modification, was investigated during experimentation. Figure 2.8 presents a picture of the final electromagnet array mounted in place around the test section.

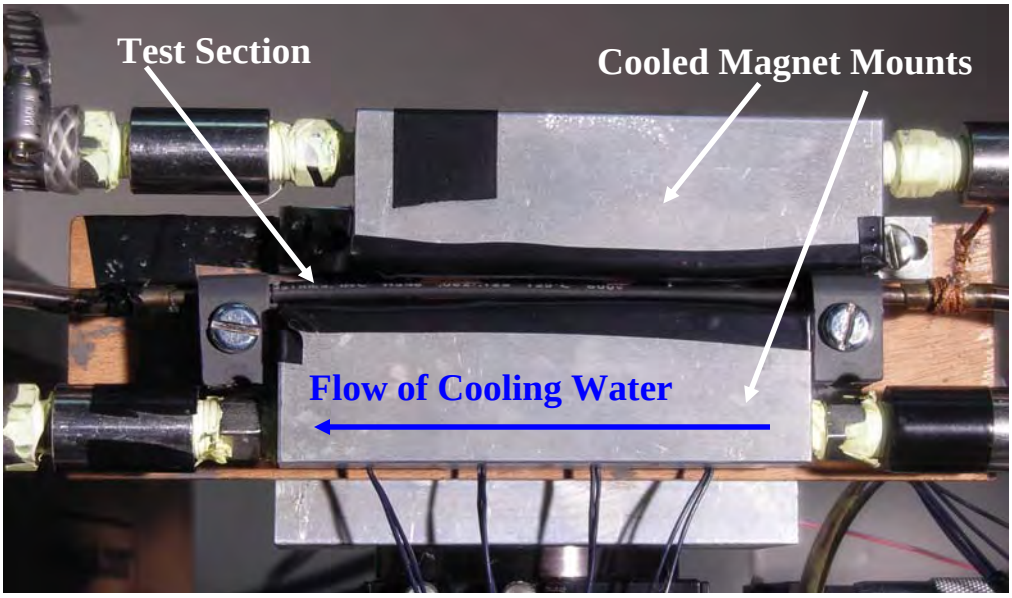

Figure 2.8: Picture of Electromagnet Array

The electromagnets were powered by power amplifiers that referenced a control signal generated within a LabVIEW virtual instrument. The LabVIEW program controlled the electromagnets with a square wave, alternatively exciting the lower and upper arrays. The frequency of the alternating activation of upper and lower magnets, as well as the power applied to the array, was controllable from the LabVIEW program. Additionally, a rest period between the activation of the opposing magnet array could be incorporated, effectively changing the duty cycle of the magnet activation function. The enhancement technique's sensitivity to variations in activation frequency, field strength and duty cycle was investigated during experimentation.

3. Experimental Procedures and Results

3.1
Overview

Many parameters of the enhancement technique under investigation were believed to potentially affect its performance, and were varied during experimentation. Properties of the electromagnet array, like the magnet switching frequency, duty cycle and field strength were manipulated, in addition to properties of the fluid system, including the flowrate, particle size and material. Trials using pure water as the heat transfer fluid were conducted to provide a baseline of comparison, and to validate the experimental apparatus and procedure against accepted correlations. The coefficient of convective heat transfer, a value which effectively summarizes the transfer of energy due to convection, was calculated and compared between experimental trials.

3.2
Calculating the Coefficient of Convective Heat Transfer

In order to determine the effectiveness of the heat transfer enhancement technique, the coefficient of convective heat transfer was experimentally determined and compared for both enhanced and non-enhanced trials. The experimental apparatus was designed to facilitate these calculations by establishing a condition of uniform heat flux into the fluid in the test section. Through resistive heating, the test section is uniformly heated by the application of an electric current across its length. The heat transfer analysis is conducted assuming minimal axial conduction, free convection to the ambient, or heat transfer by radiation. These assumptions are validated by analytically comparing the relatively large internal forced convection coefficients to the transfer coefficients for the other modes of energy transport. Thus, all the energy supplied to the test section is assumed to be transferred to the fluid by convection. From the principle of conservation of energy, assuming no changes in latent energy, no axial conduction or losses to

the ambient, and steady state conditions, the simplified steady-flow thermal energy equation can be written:

$$q_{conv} = m_{dot}\, c_p (T_{fluid,O} - T_{fluid,I}) \quad [2]$$

where q_{conv} is the heat transferred by convection, m_{dot} is the mass flow rate of the working fluid, c_p is the specific heat of the working fluid and $T_{fluid,O}$ and $T_{fluid,I}$ are the fluid temperature at the test section outlet and inlet, respectively.

Equation [2] is valid for flows of incompressible liquids with negligible viscous dissipation, and is applicable to the conditions of the experiment. Applying equation [2] to a differential control volume of an internal flow, as shown in Figure 3.1, it follows that:

$$\delta q_{conv} = m_{dot} c_p [(T_{fluid} + dT_{fluid}) - T_{fluid}] \quad [3]$$

where δq_{conv} is the heat transferred to an infinitesimal control volume by convection and dT_{fluid} is the change in fluid temperature across that control volume.

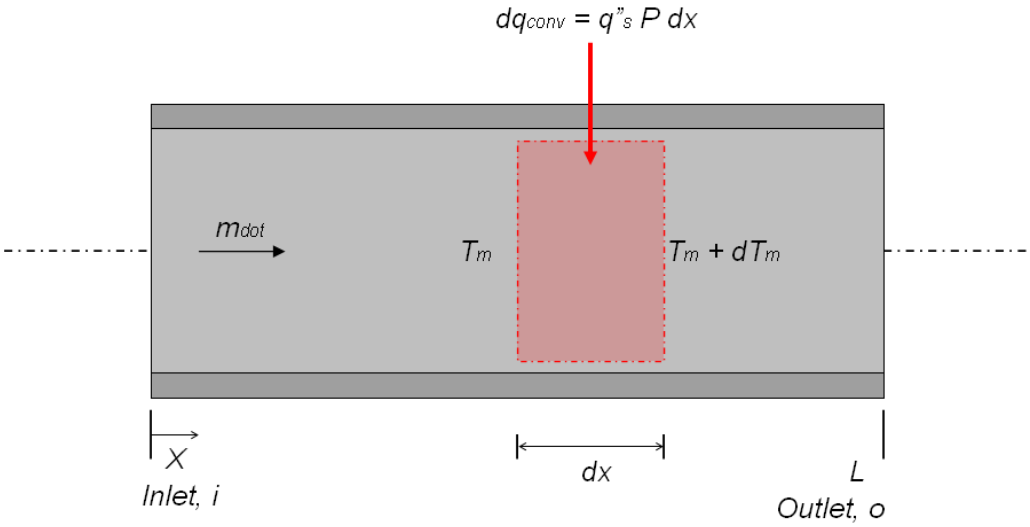

Figure 3.1: Control Volume for Internal Flow in a Tube

When simplified, equation [3] becomes:

$$\delta q_{conv} = m_{dot} c_p dT_{fluid} \quad [4]$$

The test section is heated through resistance heating, whereby the resistance of the material converts an electric current across the tubing to thermal energy. Because this process is a volumetric effect, the test section is heated uniformly, applying a constant surface heat flux to the fluid. Equation [5] shows that the heat applied to a differential control volume is equal to this constant heat flux multiplied by the volume's surface area,

$$\delta q_{conv} = q_s'' P dx \quad [5]$$

where q_s'' is the heat flux applied to the control volume, *dx* is the length on the control volume and the volume's perimeter is represented by $P = \pi D$

While the control volume is at steady state conditions, its temperature remains constant because the heat generated within the test section, [5], equals the heat transfer into the fluid, [4]. Combining these equations yields:

$$\frac{dT_{fluid}}{dx} = \frac{q_s'' P}{m_{dot} c_p} \quad [6]$$

Integrating equation [6] under conditions of constant surface heat flux, it is determined that the temperature of the heat transfer fluid is linearly related to position[21]:

$$T_{fluid}(x) = T_{fluid,I} + \frac{q_s'' P}{m_{dot} c_p} x \quad [7]$$

Assuming a constant surface heat flux, the local convective heat transfer coefficient at any position, $h_{conv}(x)$, can be calculated from the difference in temperature between the fluid and the heat transfer surface, T_{tube}, [8]:

$$h_{conv}(x) = \frac{q_s''}{T_{tube}(x) - T_{fluid}(x)} \quad [8]$$

Figure 3.2 presents the tube and fluid temperature distributions expected from an internal flow subjected to a constant surface heat flux. The temperature of the fluid is linear, as determined by [7], and the tube temperature becomes linear after it reaches a fully developed region. In the initial length of the tube known as the developing region, layers of laminar flow are still forming on the heat transfer surface, and the rate of heat transfer is changing with position. Farther down the length of the tube, the flow reaches a fully developed regime and tube temperature becomes linearly related to position. In this fully developed region, the temperature difference between the tube and the fluid, and thus the coefficient of convective heat transfer, reaches a constant value.

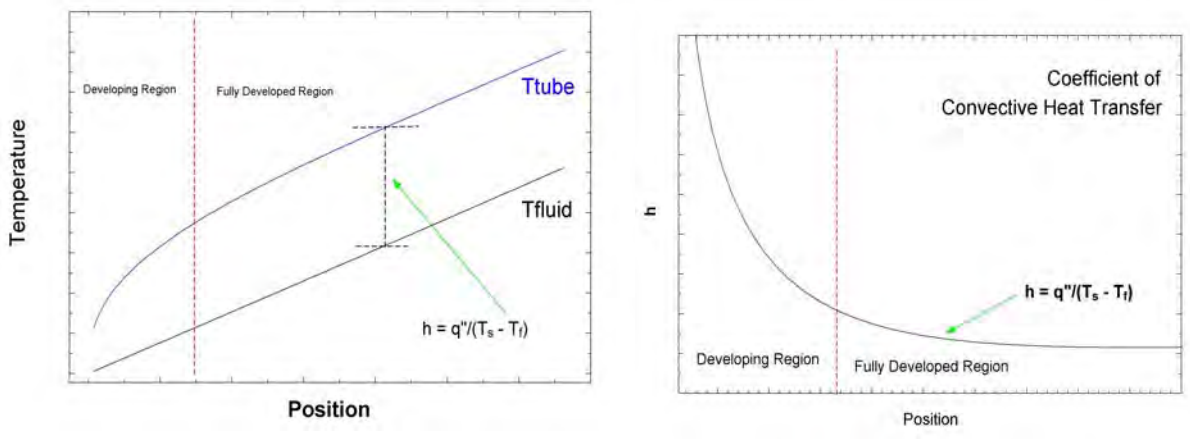

Figure 3.2: Profiles of Tube and Fluid Temperature, left, and Coefficient of Convective Heat Transfer, right in Internal Flow under Uniform Heat Flux Condition

The experimental apparatus was designed to facilitate the calculation of the coefficient of convective heat transfer at any axial position by utilizing equation [8]. The temperature of the tube, $T_{tube}(x)$, at every position along the test section was measured by the infrared camera, and the temperature of the fluid at every position was calculated using equation [7] from the temperatures at the inlet and exit of the test section. The heat flux applied to the test section, q_s'',

is determined by dividing the total heat absorbed by the fluid, calculated from equation [2], by the heat transfer surface area.

3.3
Baseline Trials: Water

Experimentation investigating the performance of this novel enhancement technique began with trials to validate the experimental apparatus and procedure. Baseline trials, without any attempted enhancement, were conducted with pure water as the heat transfer fluid. Experimental data was used to calculate the coefficient of convective heat transfer, and was compared to the coefficient of heat transfer expected from an accepted correlation for heat transfer in laminar internal flows.[21]

Baseline experimentation began using the 1100 micron diameter test section. After the calibration of the data acquisition system, data was collected at a range of flowrates and heating inputs. The results of these preliminary baseline trials showed areas of inaccuracy in the experimental apparatus, and motivated an iterative redesign of components that were introducing error. Specifically, these initial tests identified two large sources of experimental error: heat was escaping the test section through unaccounted paths, and the preparation of the tube surface for thermography did not produce clean infrared images.

The calculations used to determine the experimental coefficients of heat transfer operate on the assumption that all the heat supplied to the test section is transferred into the fluid. Heat leaving the test section through other paths is unaccounted for in these calculations, and introduced an experimental error. To observe this source of error, a diagnostic test was conducted where hot water was pumped through the unheated test section.

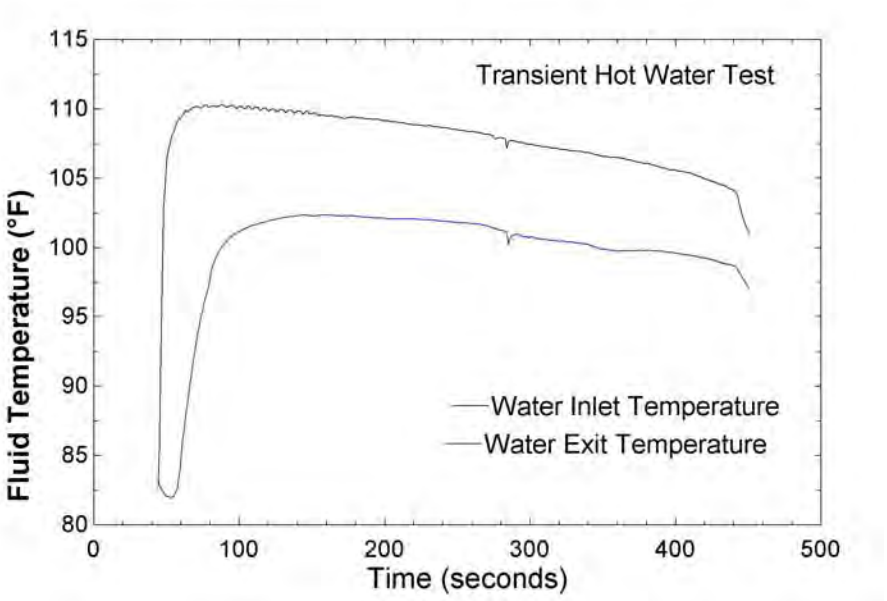

Figure 3.3: Inlet and Outlet Fluid Temperatures over Time Showing Unaccounted Heat Loss

After reaching equilibrium, a test section with no external heat losses would exhibit identical inlet and outlet temperatures. However, the inlet temperature was approximately 6% higher than the outlet temperature during diagnostic testing of the initial design. Figure 3.3 presents the fluid temperatures over time capturing the loss of heat from the test section.

After examining the experimental apparatus, conduction from the test section into the original aluminum mounts was determined to be the most likely path of unaccounted heat transfer. The mounts were redesigned and manufactured from PVC, a thermally insulating material. This design modification significantly reduced the differential between the fluid inlet and exit temperature during diagnostic tests, mitigating this potential source of error.

The second significant source of experimental error is associated with the quality of the infrared images of the test section. The highly reflective surface of the untreated, metallic test section is not conducive to infrared thermography. In order to get accurate temperature information from these infrared images, the test section was coated with a thin layer of flat paint to provide a surface of consistent emissivity. However, after repeated heating and cooling, this paint layer no longer provided a consistent surface. The tube temperature profile taken from these infrared

images was inconsistent, marked by inexplicable hot and cold spots along the length of the tubing, shown in Figure 3.4, below. This problem was addressed by using a thin layer of electrical tape, instead of flat paint, to provide a surface of constant optical properties. This tape, which could potentially act as an insulator for the test section, introduces a minor lag as the test section is heated to a steady state temperature, but does not affect that steady state value detected by the IR camera. In later modifications, the layer of electrical tape was replaced with heat shrink tubing to accomplish the same purpose.

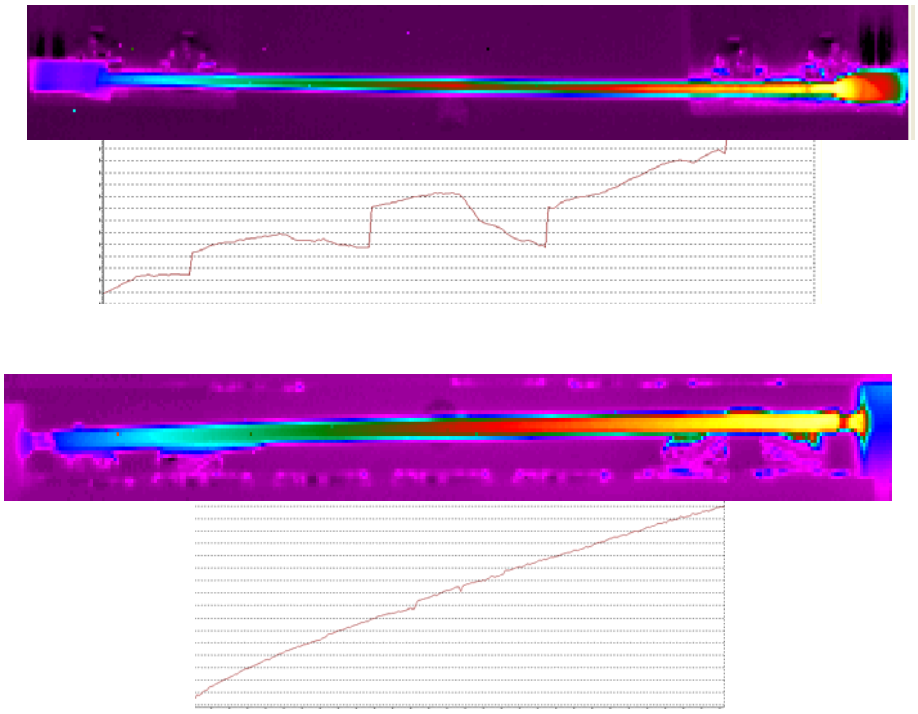

Figure 3.4: IR Image and Tube Surface Temperature of Test Section Before, above, and After, below, application of Electrical Tape

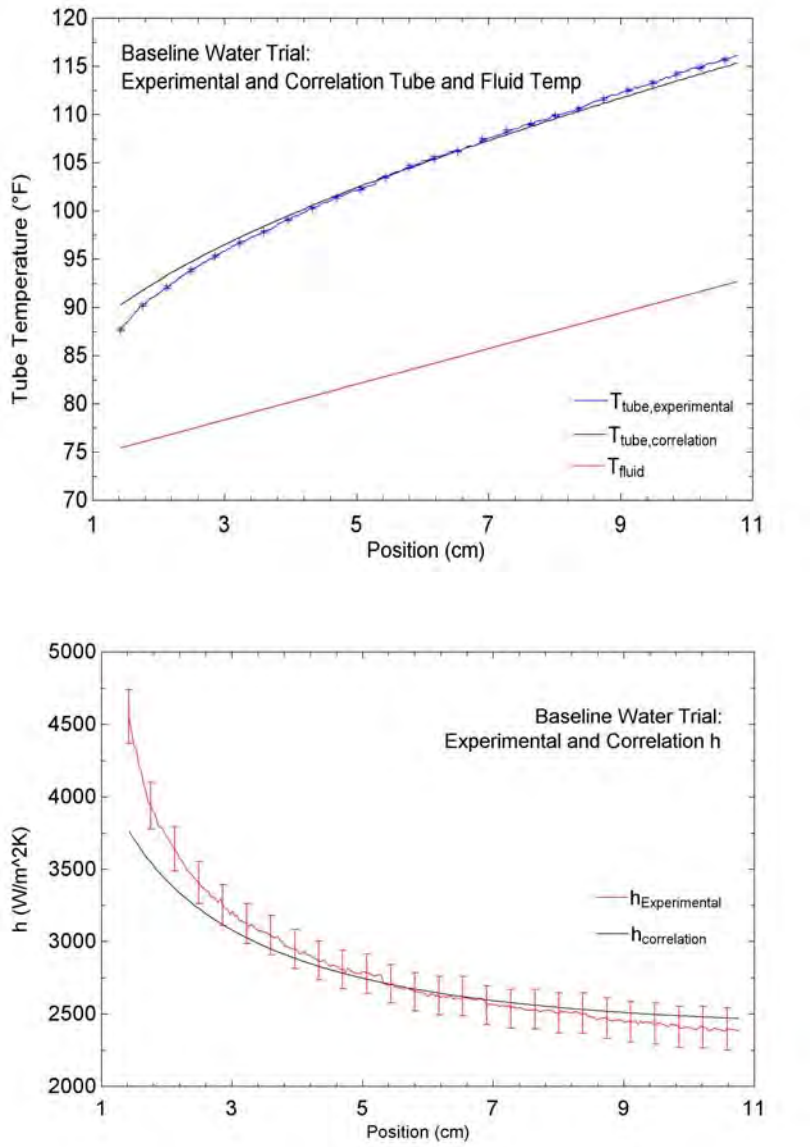

Figure 3.5: Experimental and Theoretical Coefficients of Convective Heat Transfer, below, and Tube and Fluid Temperatures, above, for Baseline Trial

After using preliminary baseline trials to diagnose and remediate major sources of error, the experimental apparatus produced data in close agreement with the theoretical correlation, validating the accuracy of the apparatus and procedure to measure heat transfer coefficients. In a baseline trial with water pumped through the 1100 micron test section at 900 mL/hr, the coefficient of convective heat transfer was calculated within the experimental uncertainty of the theoretical correlation. Figure 3.5 presents these experimental and theoretical *h* values, in

addition to fluid and tube temperature profiles developed from theoretical and experimental trials. Table 2 presents the experimental uncertainty from the baseline water trials.

Table 2
Baseline Water Trial: Experimental Uncertainty

Measurand	Absolute Uncertainty	Value	Relative Uncertainty
Inlet Fluid Temperature	0.0523 deg F	72.84 deg F	0.07%
Outlet Fluid Temperature	0.7283 deg F	95.03 deg F	0.77%
Tube Surface Temperature	0.15 deg F	87.73 - 115.5 deg F	0.17 - 13%
Flowrate	1 ml/hr	900 ml/hr	0.11%

Table 2: Baseline Water Trials: Experimental Uncertainty

3.4
Experimental Trials: Magnet Integration

Having validated the experimental apparatus through baseline trials using water alone, apparatus modification necessary for enhanced trials began. The most significant modification required was the integration of the dual electromagnet arrays. The initial electromagnet arrays consisted of rows of 6 and 7 magnets in PVC mounts offset above and below the test section, as shown in Figure 2.2. Before experimentation, baseline tests were conducted to determine the electromagnet array's effect on the performance of the apparatus. With water flowing through the tubing, the temperature of the test section consistently increased locally around the magnets while they were activated. This magnet heating problem was further exacerbated when the magnets were operated at higher powers or frequencies. Possible explanations for this unexpected heating included eddy current heating, by which the alternating magnet fields induce currents in the metallic test section, which thereby heat the tube through resistance heating. However, the heating was also observed when the magnets were operated continuously, with DC power, eliminating the viability of eddy current heating.

The electromagnets used in the apparatus dissipate a significant amount of heat during operation, and because the field strength encountered by an object is proportional to the distance from the electromagnet, the magnet array had to be very close to the test section. However, the magnets dissipated a significant amount of heat into the enclosed space surrounding the test section. This effect is attributed as the cause of the change in tube surface temperature during magnet

operation. The magnet heating effect is observed below, in Figure 3.6, which presents infrared images of the heated test section with the magnets operating at their rated power. Each image was taken at a 30 second interval.

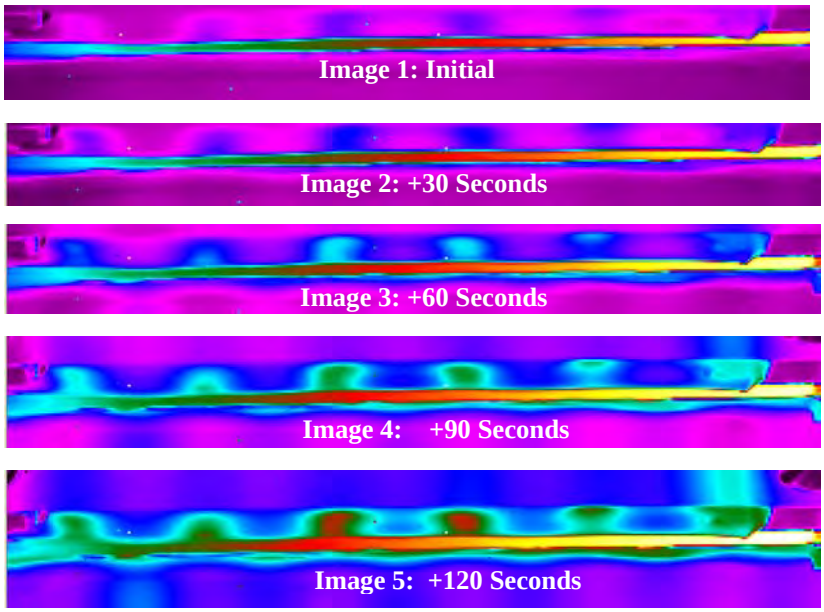

Figure 3.6: Magnet heating effect in initial electromagnet array

The heating due to the magnets was mitigated by actively cooling the magnet array. The magnet mount was redesigned out of aluminum and a chiller was used to pump cooling water through a channel bored behind the magnets. The final electromagnet array design is presented in section 2.6. The modifications to the electromagnet array significantly reduced the heat absorbed by the test section due to the electromagnets, demonstrated by the plots below. Figure 3.7 shows the reduced local heating around the electromagnets in trials where the magnets are actively cooled. Water was pumped through the heated test section, and the magnets were activated at increments of their rated power. The plots presented below in Figure 3.7 show the increase in temperature above the baseline value for trials with the electromagnets at their rated power, twice their rated power, and three times their rated power when the magnet array both was and was not actively cooled.

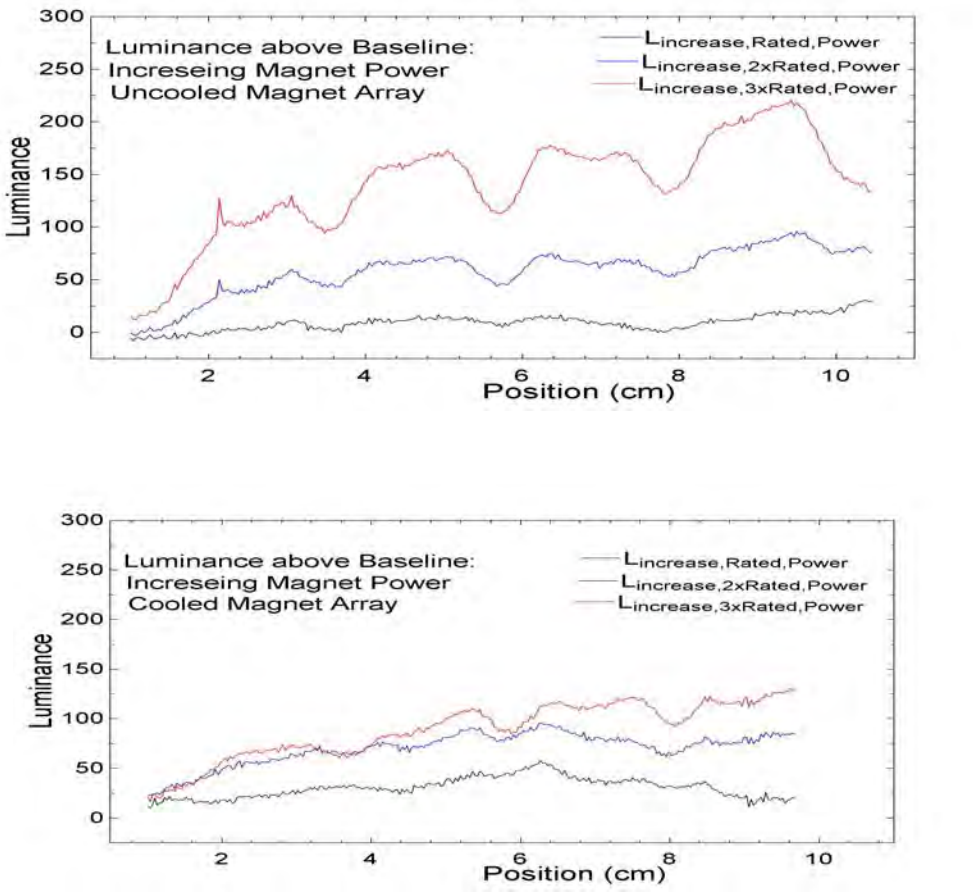

Figure 3.7: Differential Temperature Plots Demonstrating Magnet Heating Effect Reduced When Actively Cooling Magnets

3.5

Experimental Trials: Fe_3O_4 Suspension

Having mitigated the test section heating due to the electromagnet array, experimental trials were conducted using a Fe_3O_4 suspension as the heat transfer fluid. A 5% by weight suspension was prepared by using bath sonication to disperse 50-nm iron oxide powder in deionized water. This concentration was used in the conventional scale demonstration of the enhancement technique. Baseline tests of the suspension, using no magnetic enhancement, were conducted and compared against water tests to determine any difference in performance between the suspension and pure water. These initial unenhanced tests, across a range of flowrates, showed no significant

variation in thermal performance between the suspension and water in the absence of applied magnetic fields. Figure 3.8 presents representative data from these trials, and only shows variation in tube temperature within the uncertainty of these measurments for comparable water and Fe_3O_4 suspension trials. This data suggests that, at the concentrations tested, the dispersion of iron oxide nanoparticles does not significantly influence the thermal characteristics of deionized water. While nanometer-scale particle laden suspensions are being investigated for their potential to anomalously increase fluid thermal conductivity, the lack of conductivity enhancement observed here supports similar negative findings by other researchers.[22]

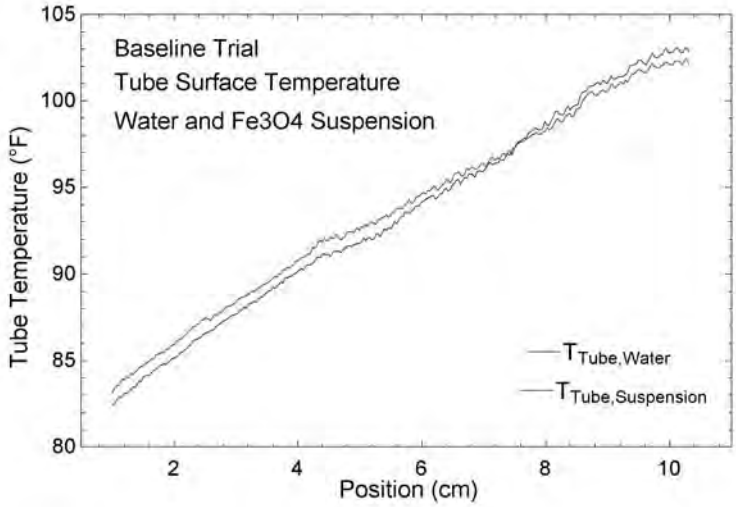

Figure 3.8: Tube Temperature Profiles for Non-enhanced Trials using Water and Fe_3O_4 Suspension

Having observed that the suspension, when not acted upon by the electromagnets, produced the same tube temperature profile as its pure base fluid, enhanced trials were conducted, applying the alternating magnetic fields to the suspension. Tests using the Fe_3O_4 suspension employed a range of magnet activation frequencies and power levels, and various flowrates, and although visual observation through glass tubing confirmed the technique's modification of the flow regime, an increase in the rate of heat transfer was not observed. Tube surface temperature was observed to increase with time while the magnets were activated, however, a comparable increase in tube temperatures were observed in trials using pure water and the same experimental procedure, as shown in Figure 3.9. Each line in these plots represents data at 15 second intervals.

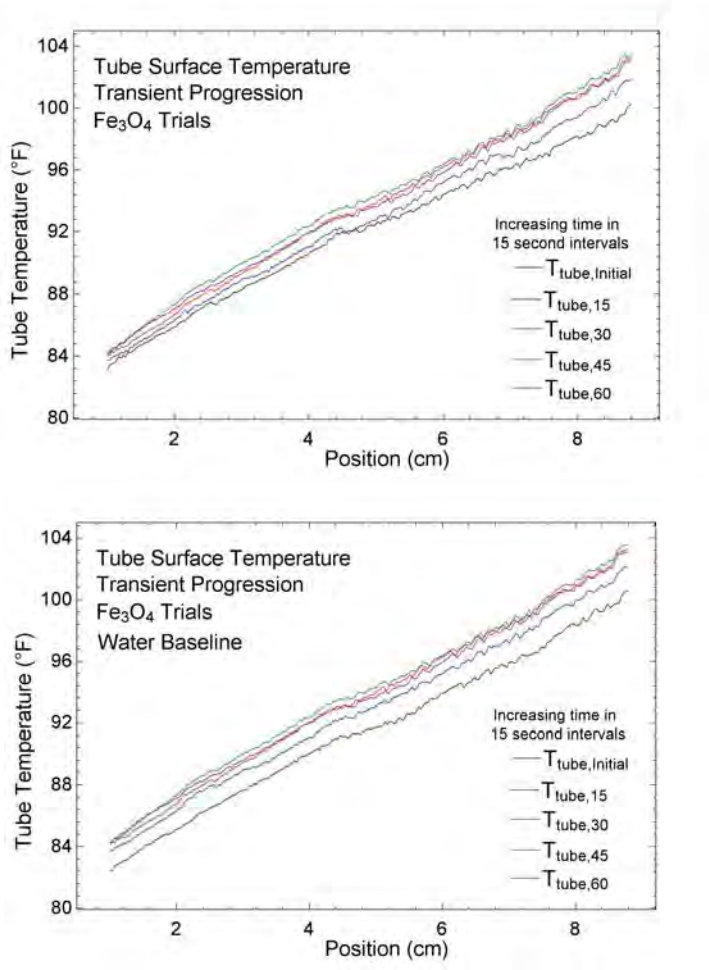

Figure 3.9: Tube Temperature Profile: Fe_3O_4 Suspension, above, and Pure Water, below.

Comparing the tube temperature at specific intervals from water trials to the Fe_3O_4 data, it was determined that the tube surface experienced the same rate of heating in both cases, shown below in Figure 3.10. This heating over time was likely caused by a residual influence from the magnet array. The transient nature of this effect was mitigated when considering data at the same time from initial magnet activation from both Fe_3O_4 and water trials. When taking the transient tube heating into account in this way, the enhancement technique was shown to have little effect on the tube surface temperature. Figure 3.10 also presents the coefficients of heat transfer for trials with both water and the Fe_3O_4 suspension, with inconsistencies within the experimental uncertainty.

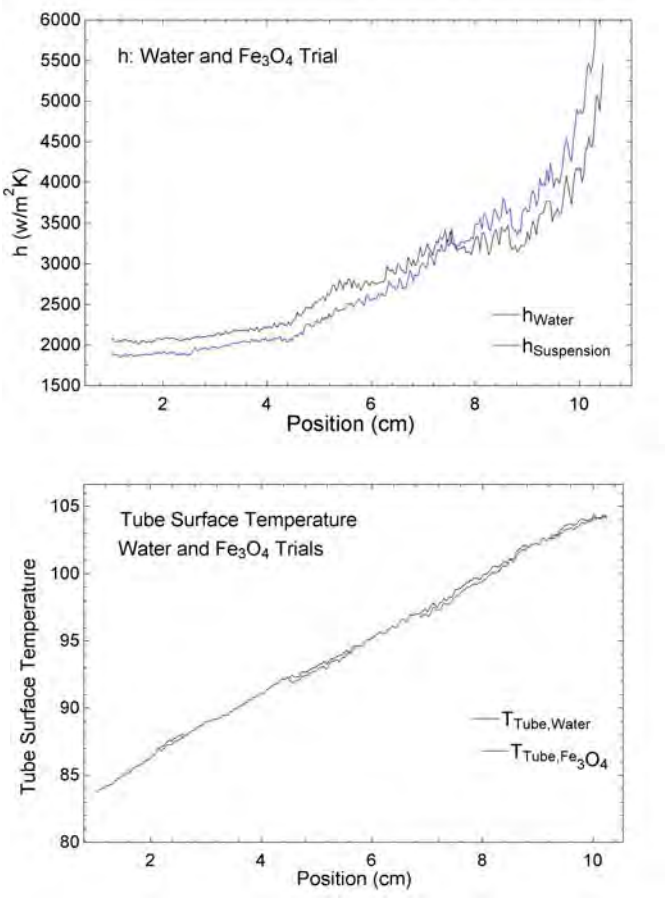

Figure 3.10: Tube Temperature, below, and h Profile, above: Fe_3O_4 Suspension and Pure Water

3.6

Experimental Trials: Surfactant-Stabilized Fe_3O_4 Suspension

During experimentation with the Fe_3O_4 suspension, the suspension was observed to have an inconsistent concentration over time, even after particle dispersion through bath sonification. During experimental trials, the iron oxide particles suspended in the fluid settled out, resting in the syringe of the pumping system, and the fluid was marked by an inconsistent color leaving the test section. In order to reduce the potential effects of transient particle concentration and to increase the consistency of the experimental procedure, the heat transfer fluid was modified to increase the stability of the suspension. A review of the literature suggested that higher and more prolonged levels of sonication during fluid preparation could successfully decrease particle size, increasing suspension stability.[23] A probe sonicator was used to apply higher levels of acoustic energy, and was moderately more effective than the bath sonicator used previously. Compared to the bath sonicator, the probe prepared a suspension displaying a color and consistency indicative of a smaller particle size. Regardless of the extent of sonication, however, the particles still settled out of the fluid, displaying the suspension's persistent lack of stability.

A review of nanoparticle literature suggested that these results were not uncommon, and identified a potential solution.[24-25] When preparing nanoparticle suspensions, surfactants are often used to modify the surface properties of the particles, reducing the inter-particle forces that promote aggregation and sedimentation. The surfactant's ability to affect the particle's solubility is strongly dependent on the nature of the particle material; a given surfactant will not be effective in all situations. Sodium polyacrylate was used as a surfactant for the Fe_3O_4 system because its effect on this material was documented in the literature.[26] The Fe_3O_4 suspension prepared using this surfactant displayed a marked increase in stability, and maintained a nearly homogeneous consistency indefinitely. While the increased suspension stability was promising, it is important to note that to achieve the anticipated flow modification, the suspension should not behave homogeneously when acted upon by the magnets. The particles are expected to come out of suspension when drawn to the heat transfer surface, but should disperse into the bulk flow when released by the magnetic field.

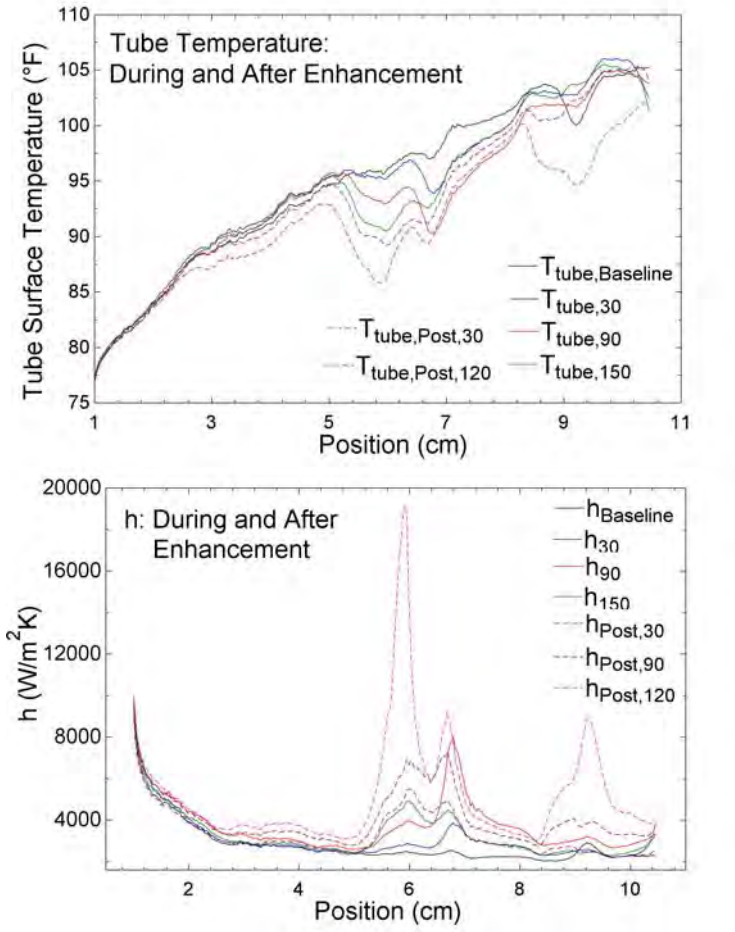

Figure 3.11: Tube Temperature and *h* Profiles for Enhanced Trials: Surfactant-Stabilized Fe_3O_4 Suspension at 1 Hz: Transient Images During and After Magnet Activation

Experimental trials across a range of flowrates, magnet activation frequencies, duty cycles, and power levels were conducted using the surfactant-stabilized Fe_3O_4 suspension. Modification to the tube surface temperature profile was observed during this experimentation; however, it did not behave as expected. In repeated trials, a reduced tube temperature profile was observed when operating the magnets at a switching frequency of 1 Hz. However, this enhancement not only unexpectedly persisted past the deactivation of the magnet array, it increased in effectiveness. The decreasing tube temperature drove up the *h* values with time, which reached a maximum average increase of 86% over the initial values at 120 seconds after magnet deactivation. Figure 3.11 presents representative data for these trials, demonstrating the persistent tube temperature

modification and increased coefficient of heat transfer. This data was taken during a trial with a flowrate of 500 mL/hr, heating power of 8.76 W, and magnet switching frequency of 1 Hz.

It is believed that the persistence of the tube temperature modification observed in Figure 3.11 is due to an unexpected modification of the flow regime. The enhancement technique relies on the electromagnets to attract the suspended particles to the tube wall, and it was expected that a combination of the hydrodynamic forces due to the flow and the activation of the opposing electromagnet would effectively remove particle aggregations from the tube surface. This behavior was seen in the conventional scale demonstration, and was observed when inspecting the modification of the flow of the un-stabilized Fe_3O_4 suspension in a 1.4 mm glass tube. However, the application of the surfactant to the suspension changed its performance, causing aggregations that formed in the presence of a magnetic field to persist past the field's removal, as observed in Figure 3.12.

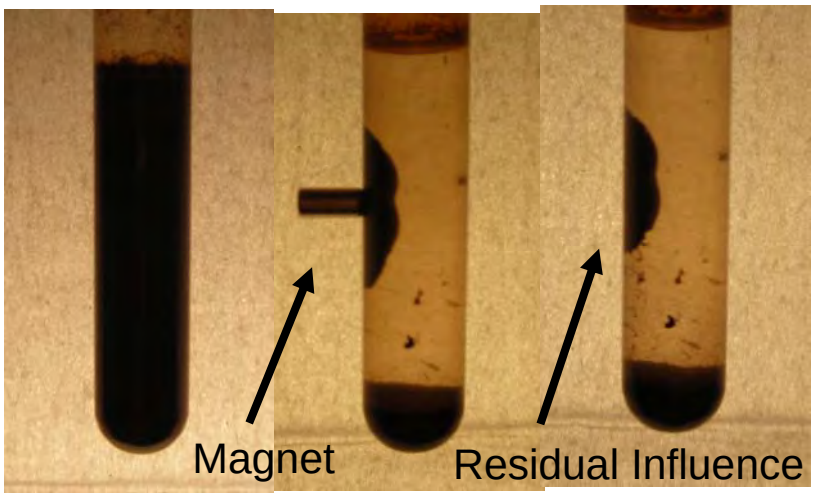

Figure 3.12: Demonstration of Residual Magnet Influence in Fe_3O_4 Suspension

It is theorized that the residual magnet influence on the suspension caused particle aggregations to form during magnet activation, and to grow after the magnets had been powered off. Figure 3.12 demonstrates the creation of an F_3O_4 particle aggregation in the presence of a magnetic field, and its persistence after the removal of the magnetic field. Aggregations formed in the test section served to reduce the tube area, increasing fluid velocity, and to disrupt the laminar flow condition within the tubing, resulting in the observed decrease in tube surface temperatures. These aggregations were also manifested in a trend of increasing pressure across the test section,

presented in Figure 3.13. The differential pressure trends upward during the first minute the magnets are activated, and reaches a steady value. However, the pressure jumps considerably when the magnets are deactivated after 3 minutes. The maximum increase in pressure, to 32% above initial values, corresponds to the dramatic reduction in tube temperature observed in Figure 3.11. Also note, the underlying cyclic variations in pressure observed in Figure 3.13 are related to the speed of the stepper motor driving the syringe pump.

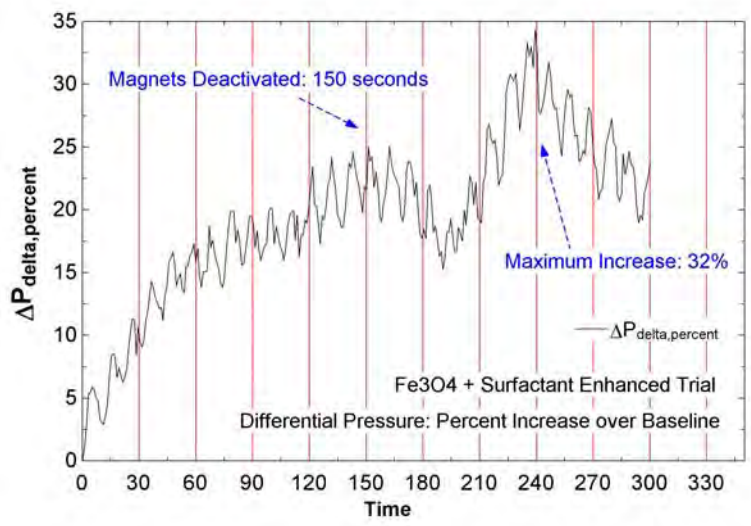

Figure 3.13: Differential Pressure of Surfactant-Stabilized Fe_3O_4 Suspension across Test Section at 1 Hz Magnet Activation

3.7

Experimental Trials: Fe Suspension

The anticipated flow manipulation was observed with the Fe_3O_4 suspension, yet the heat transfer enhancement behaved unexpectedly. Therefore, trials were conducted on an iron (Fe) based suspension to determine the effect of particle material on the technique. This material was selected because iron particles were dispersed in the suspension used to demonstrate the technique on conventional scales.[27] A 5% (by weight) suspension was prepared by dispersing 6 micron Fe particles in deionized water using bath sonication. These larger particles fell out of suspension more readily than the smaller Fe_3O_4 particles, but were more strongly reactive to an

applied magnetic field and did not form the persistent particle aggregations observed in the surfactant-stabilized Fe_3O_4 suspension. To mitigate the effects of the suspension's poor stability, the experimental apparatus was modified to test the suspension in a closed loop system using a peristaltic pump as shown in Figure 2.7. In all of the tubing and connections aside from the test section, this closed loop system maintained a relatively high flowrate, higher than the particle's critical settling velocity, below which the particles would fall out of suspension.

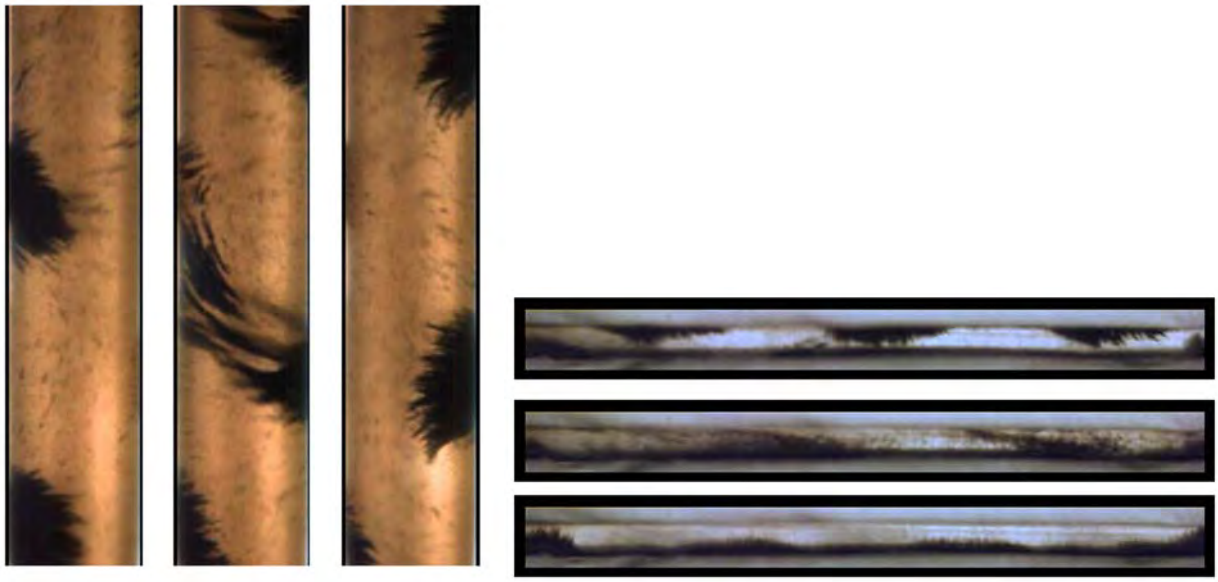

Figure 3.14: Visual Observation of Flow Modification in Current Experiment, right, and Conventional Scale Demonstration, left

Visual observation of the flow through glass tubing with a high speed camera confirmed that the enhancement technique established the flow manipulation anticipated from the conventional scale demonstration. Figure 3.14 presents these observations, showing the particles attracted to one surface, then released into the flow, then attracted to the opposite surface for both the trial conducted here and the conventional demonstration.

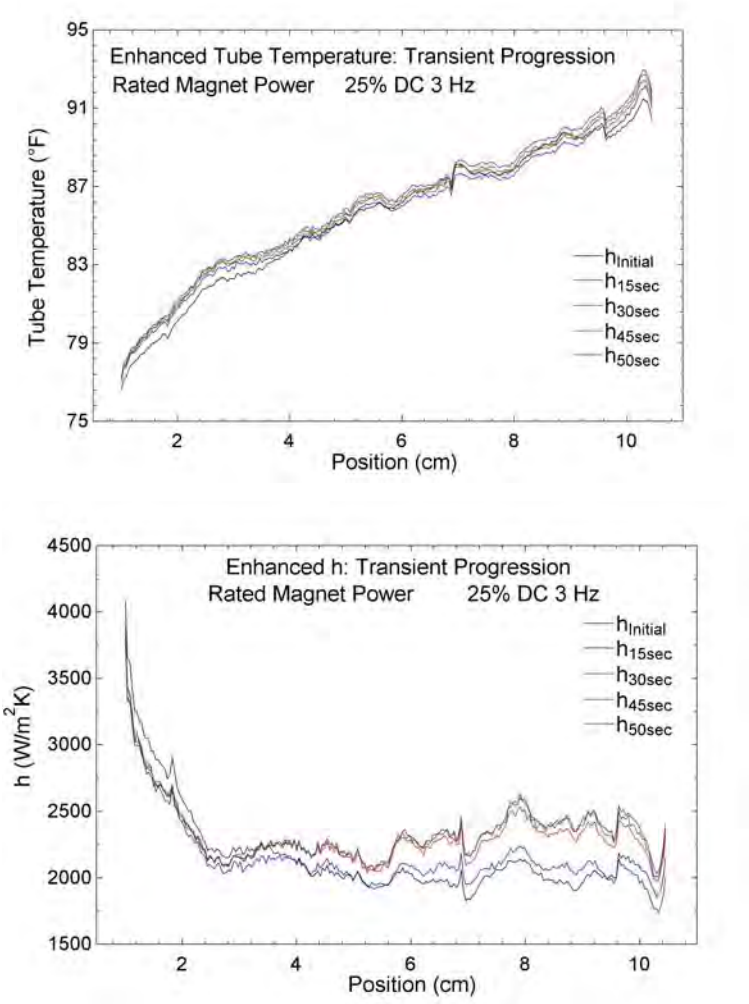

Figure 3.15: Tube Surface Temperature Profile, above, and *h* Profile, below, for Most Effective Fe-Suspension Trial

In the experimental Fe trials, the flow modification due to the technique resulted in marked heat transfer enhancement over time. Representative data is presented in Figure 3.15, and shows the tube temperature and coefficient of heat transfer profiles with increasing time for the trial demonstrating the maximum enhancement. This trial, conducted with the electromagnet arrays operating at their rated power and a frequency of 3 Hz with a 25% duty cycle resulted in a 23% increase of the average *h* value after 60 seconds of magnet activation.

Figure 3.15 does show, however, that the enhancement was manifested in an unexpected fashion. In these trials, the tube surface temperature increased with time, which might be seen as an

indicator of negative enhancement. However, understanding the difference between the closed loop pumping system used here, and the syringe pump system previously used explains the enhancement calculations. In the syringe pump system, the flowrate through the test section is constant because the test section is the only fluid path. However, the peristaltic pump used in the closed loop system has a minimum flowrate roughly an order of magnitude larger than the flowrates used in experimentation. To reduce the flowrate through the test section, additional tubing was connected parallel to the test section. The flowrate through the test section for baseline trials was calculated from the pump output and the area of the test section compared to the total area of all parallel fluid paths. However, any increase in differential pressure caused by the enhancement technique results in a reduction in flowrate through the test section. With the constant heat flux still applied, the reduced flow through the test section results in a larger fluid temperature. Thus, in the closed loop system, an increase in tube temperature did indicate enhancement because the fluid temperature also increased, reducing the temperature difference between fluid and tube and increasing *h*.

The technique's potential to reduce the flow through the test section was demonstrated at higher magnet duty cycles. Increasing the magnet duty cycle decreases the lag between the activation of the opposing magnet array. Tests conducted at 75% and 100% duty cycles saw the tube partially or completely obstructed and tube temperature climb dramatically with time, as reported in Figure 3.16.

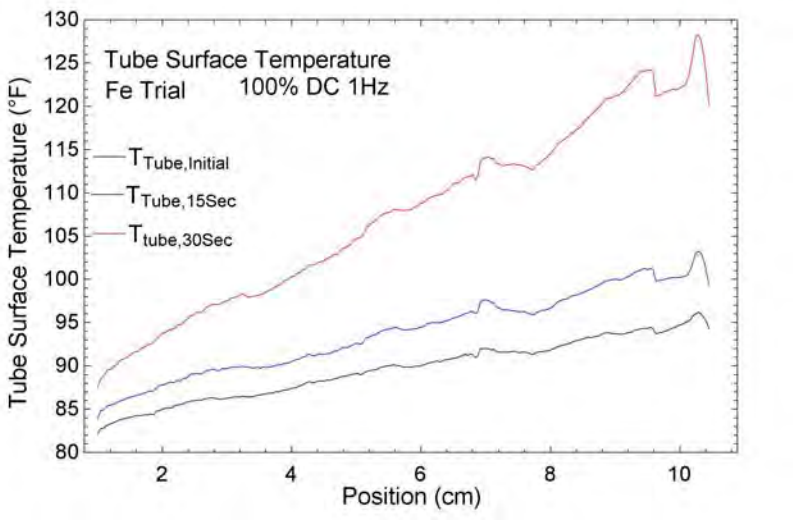

Figure 3.16: Tube Surface Temperature Profile: Obstructed Tube: Fe-Suspension at 100%DC

For all the frequencies tested, the technique produced a larger increase in *h* when operating at lower duty cycles. Data summarizing the sweep of parameters is presented below in Table 2.

Percent increase of *h* over baseline values for tests at various parameters

Duty Cycle		25%
	Magnet Power	
Frequency	1x	3x
1Hz	14.27	2.15
3Hz	23.14	7.87
5Hz	11.88	15.04

Duty Cycle	50%
	Magnet Power
Frequency	1x
1Hz	13.17
3Hz	12.72
5Hz	9.92

Duty Cycle	75%
	Magnet Power
Frequency	1x
1Hz	14.38
3Hz	Excessive Heating
5Hz	Excessive Heating

Duty Cycly	100%
	Magnet Power
Frequency	1x
1Hz	Excessive Heating
3Hz	Excessive Heating
5Hz	Excessive Heating

Table 3: Percent Increase of *h* over Baseline Values for Fe Tests at Various Parameters

The data from the Fe trials composing the sweep of parameters presented above suggests that the electromagnet array parameters, including activation frequency, magnet power and duty cycle all influence the performance of the enhancement technique. Definitively, this data concludes that there is a maximum duty cycle near 75% above which the technique clogs the tubing and cuts off flow to the test section. Concurrently, the data suggests that higher levels of magnet power significantly inhibit the technique's effectiveness. Magnet activation frequency is seen to influence the technique's performance, however its effect changes across the range of duty cycles tested. The technique's sensitivity to parameter variations, demonstrated in this limited data, motivates a more thorough and conclusive parameter search in future work.

4. Conclusions

The intent of this project was to design and fabricate an apparatus, and to implement an experimental procedure to determine the viability of a novel convective heat transfer enhancement technique in mini- and micro-channel flows. The apparatus and procedure were validated by accurately determining the coefficient of convective heat transfer, *h*, in a 1.1 mm heated test section. Within the experimental uncertainty, the experimental values of *h* for baseline water trials agreed with those developed from an accepted correlation describing laminar internal forced convection.

Trials demonstrating the enhancement technique in a 1.1 mm diameter tube were conducted using three different suspensions of Fe and Fe_3O_4 particles. Visual observation of all three suspensions in a 1.4 mm glass tube confirmed that the technique effectively modified the flow regime. The alternating magnetic fields caused the particles suspended in the heat transfer fluid to oscillate between the tube walls, disrupting the laminar flow conditions in the tubing. This flow modification is consistent with that observed in the conventional scale demonstration of this enhancement technique.

While the anticipated flow modification was observed using all three suspensions, enhanced trials revealed the technique's varying effectiveness on each suspension's thermal performance. Enhanced tests conducted on the initial Fe_3O_4 suspension failed to demonstrate any significant heat transfer enhancement. While these tests did show changes to the tube surface temperature over time, the same changes were observed when testing with pure water and were attributed to heating caused by the electromagnet array.

Noting the sedimentation of Fe_3O_4 particles from the initial suspension, a surfactant was used to increase its stability. The surfactant-stabilized Fe_3O_4 suspension displayed a marked increase in stability, maintaining a nearly homogenous consistency indefinitely. However, aggregations that formed from the stabilized solution in the presence of magnetic fields were shown to persist after these fields were removed. Experimental tests using this suspension documented significant local decreases in tube temperature; however, this effect persisted and intensified past the deactivation

of the electromagnets. This effect was most likely caused by particle aggregations forming in the test section and continuing to grow after the deactivation of the magnets; a trend of increasing differential pressure supports this conclusion. While these enhanced trials resulted in an 86% maximum increase of *h* over baseline values, they demonstrated that the technique does not produce heat transfer enhancement in the stabilized-Fe_3O_4 suspension in the manner observed in the conventional scale demonstration.

The enhancement technique was also tested using a Fe-particle suspension, employing particles of the same metal used in the conventional scale test. These particles were significantly larger than those used in the Fe_3O_4 suspensions, and displayed a much stronger reaction to applied magnetic fields. Additionally, the Fe suspension did not form the persistent aggregations observed when testing the stabilized Fe_3O_4 suspension. Enhanced trials employing the Fe suspension produced the type of flow modification and heat transfer enhancement expected from the conventional scale experiments, and demonstrated the technique's sensitivity to changes in parameters including magnetic field strength, activation frequency and duty cycle. The maximum enhancement observed resulted in a 23% increase in *h* over baseline values.

While tests on the Fe suspension resulted in the type of heat transfer enhancement anticipated, the technique's effect at small scales is an order of magnitude less than the enhancement observed at conventional scales. Unenhanced conventional scale tests developed a heat transfer coefficient of 57.5 W/m^2K and the enhancement technique increased this coefficient to 205.8 W/m^2K. On the other hand, unenhanced miniaturized tests produced coefficients of heat transfer on the order of 2000 W/m^2K while enhancement brought this value to roughly 2500 W/m^2K. The smaller relative magnitude of enhancement in the miniaturized tests is likely influenced by the significantly larger non-enhanced *h* values; the enhancement observed in conventional scale tests can be attributed to the relatively poor thermal performance in initial tests. The disparity between the unenhanced heat transfer coefficients in conventional and miniaturized experimentation is due to not only the difference in hydraulic diameter, but also the properties of the base fluids. Water, used in the miniaturized experiments, is a better heat transfer fluid than the mineral oil used in conventional scale tests.

This research represents the initial development of a heat transfer enhancement technique that, if improved upon and determined viable in future tests, could be employed in an end-use thermal management application. It is not difficult to envision the fabrication of a heat sink incorporating this technique; heat sinks featuring hydraulic diameters of this scale have been developed, and the alternating magnetic fields could be provided by electromagnets created using microfabrication techniques. However, the challenges faced throughout this research have made it clear that further developments would be required before an end-use application could be realized. Future research should be conducted using hydraulic diameters ranging between those tested here and in the conventional scale demonstration. The technique is exceptionally effective at one end of the spectrum, and marginally effective at the other; mapping its performance in the region in between will lend insight into the technique. Continuing investigations should also examine other applicable particle laden fluids, with a focus on understanding and controlling the stability of the suspension. Fluid stability was determined to significantly influence the enhancement technique's performance and complications rising from this issue, like the potential to clog or foul tubing with sedimentation from a suspension, could prove to limit the technique's ultimate viability. Finally, further investigations should also limit the parameters changed from the successful conventional scale tests. When developing the plan for the experimentation conducted in this research, two aspects of the conventional scale apparatus were changed. Not only was the test section miniaturized, but water, instead of oil, was used as the base fluid of the particle laden suspension. Future experimentation should be conducted using the water based suspensions in the conventional scale apparatus, and an oil based suspension in the miniaturized tests.

5. Endnotes

[1] Incropera, F.P., DeWitt, D.P., Bergman, T.L., and Lavine, A.S., 2007, *Introduction to Heat Transfer,* J. Wiley & Sons, Chap. 6.
[2] Steinke, M.E., and Kandlikar, S.G., 2004, "Single-Phase Heat Transfer Enhancement Techniques in Microchannel and Minichannel Flows," *International Conference on Microchannels and Minichannels.*
[3] Crowe, C., Sommerfeld, M., Tsuji, Y., 1998, *Multiphase Flowes with Droplets and Particles,* CRC Press.
[4] Hetsroni, G., Mosyak, A., Pogrebnyak,, 2002, "Effect of coarse particles on the heat transfer in a particle-laden turbulent boundary layer**,"** Int. J. Multiph. Flow, **28,**12.
[5] Choi, S., 1995, "Enhancing Thermal Conductivity of Fluids with Nanoparticles," *Developments and Applications of Non-Newtonian Flows,* ed. DA Siginer, HP Wang, pp. 99-105.
[6] Yoo, D.H., Hong, K.S., Yang, H., 2006, "Study of Thermal Conductivity of Nanofluids for the Application of Heat Transfer Fluids," *Thermochimica Acta*, **455**, 1, pp. 66-69.
[7] Yang, H., Hong, T, Choi, S., 2005, "Study of the Enhanced Thermal Conductivity of Fe Nanofluids," *Journal of Applied Science*, **97**.
[8] Eastman, J.A., Phillpot, S.R., Choi, S., Keblinski, P., 2004, "Thermal Transport in Nanofluids," *Annual Review of Materials Research*.
[9] Lee, J., Flynn, R.D., Goodson, K.E., Eaton, J.K., 2007, "Convective Heat Transfer of Nanofluids (DI Water-Al2O3) in Microchannels," *Proceedings of ASME Thermal Engineering Summer Heat Transfer Conference*.
[10] Incropera, F.P., DeWitt, D.P., Bergman, T.L., and Lavine, A.S., 2007, *Introduction to Heat Transfer,* J. Wiley & Sons, Chap. 6.
[11] Steinke, M.E., and Kandlikar, S.G., 2004, "Single-Phase Heat Transfer Enhancement Techniques in Microchannel and Minichannel Flows," *International Conference on Microchannels and Minichannels.*
[12] Murray, M.M., 2007, "Heat transfer enhancement using ferromagnetic particle laden fluid and oscillating magnetic fields," *Proceedings of the ASME/JSME Thermal Engineering Summer Heat Transfer Conference - HT 2007*, v 2, pp107-113.
[13] Lee, J.L., Flynn, R.D., Goodson, K.E., Eaton, J.K., 2007, "Convective Heat Transfer of Nanofluids (DI Water-Al2O3) In Microchannels," *Proceedings o 2007 ASME Thermal Engineering Summer Heat Transfer Conference*, 2007.
[14] Lee, J.L., Flynn, R.D., Goodson, K.E., Eaton, J.K., 2007, "Convective Heat Transfer of Nanofluids (DI Water-Al2O3) In Microchannels," *Proceedings o 2007 ASME Thermal Engineering Summer Heat Transfer Conference*, 2007.
[15] Murray, M.M., 2007, "Heat transfer enhancement using ferromagnetic particle laden fluid and oscillating magnetic fields," *Proceedings of the ASME/JSME Thermal Engineering Summer Heat Transfer Conference - HT 2007*, v 2, pp107-113.
[16] Choi, S., 1995, "Enhancing Thermal Conductivity of Fluids with Nanoparticles," *Developments and Applications of Non-Newtonian Flows,* ed. DA Siginer, HP Wang, pp. 99-105.
[17] Yoo, D.H., Hong, K.S., Yang, H., 2006, "Study of Thermal Conductivity of Nanofluids for the Application of Heat Transfer Fluids," *Thermochimica Acta*, **455**, 1, pp. 66-69.

[18] Ding, P., Pacek, A.W., 2009 "Ultrasonic Processing of Suspensions of Hematite Nanopowder Stabilized with Sodium Polyacrylate," *American Institute of Chemical Engineers Journal,* **55**, 11, p 2796-2806.
[19] Birdi, K.S., *2003, Handbook of Surface and Colloid Chemistry, 2nd Edition,* CRC Press, Chapters 6-7.
[20] Ding, P., Pacek, A.W., 2009 "Ultrasonic Processing of Suspensions of Hematite Nanopowder Stabilized with Sodium Polyacrylate," *American Institute of Chemical Engineers Journal,* v 55, n 11, p 2796-2806, November 2009.
[21]Incropera, F.P., DeWitt, D.P., Bergman, T.L., and Lavine, A.S., 2007, *Introduction to Heat Transfer,* J. Wiley & Sons, Chap. 8.
[22] Lee, J.L., Flynn, R.D., Goodson, K.E., Eaton, J.K., 2007, "Convective Heat Transfer of Nanofluids (DI Water-Al2O3) In Microchannels," *Proceedings o 2007 ASME Thermal Engineering Summer Heat Transfer Conference*, 2007.
[23] Ding, P., Pacek, A.W., 2009 "Ultrasonic Processing of Suspensions of Hematite Nanopowder Stabilized with Sodium Polyacrylate," *American Institute of Chemical Engineers Journal,* v 55, n 11, p 2796-2806, November 2009.
[24] Vékás, L., 2007"Ferrofluids: Synthesis, Structure, Properties and Applications," *New Magnetic Materials and Their Functions, European School of Magnetism*¸September 2007.
[25] Choi, C., Yang, H.S., Hong, T.K., 2007, "Study of the enhanced thermal conductivity of Fe nanofluids," Journal Of Applied Physics, v97.
[26] Ding, P., Pacek, A.W., 2009 "Ultrasonic Processing of Suspensions of Hematite Nanopowder Stabilized with Sodium Polyacrylate," *American Institute of Chemical Engineers Journal,* v 55, n 11, p 2796-2806, November 2009.
[27] Murray, M.M., 2007, "Heat transfer enhancement using ferromagnetic particle laden fluid and oscillating magnetic fields," *Proceedings of the ASME/JSME Thermal Engineering Summer Heat Transfer Conference - HT 2007,* v 2, pp107-113.

6. Bibliography

Birdi, K.S., *2003, Handbook of Surface and Colloid Chemistry, 2nd Edition,* CRC Press, Chapters 6-7.

Briscoe, B., Khan, A., Luckham, P., 1998, "Optimising the Dispersion on an Alumina Suspension Using Commercial Polyvalent Electrolyte Dispersants," *Journal of the European Ceramic Society*, **18**, 1.

Choi, S., 1995, "Enhancing Thermal Conductivity of Fluids with Nanoparticles," *Developments and Applications of Non-Newtonian Flows,* ed. DA Siginer, HP Wang, pp. 99-105.

Choi, C., Yang, H.S., Hong, T.K., 2007, "Study of the enhanced thermal conductivity of Fe nanofluids," Journal of Applied Physics, **97**.

Crowe, C., Sommerfeld, M., Tsuji, Y., 1998, *Multiphase Flowes with Droplets and Particles,* CRC Press.

Ding, P., Pacek, A.W., 2009 "Ultrasonic Processing of Suspensions of Hematite Nanopowder Stabilized with Sodium Polyacrylate," *American Institute of Chemical Engineers Journal*, **55**, 11, p 2796-2806.

Eastman, J.A., Phillpot, S.R., Choi, S., Keblinski, P., 2004, "Thermal Transport in Nanofluids," *Annual Review of Materials Research,* **34**.

Eberbeck, D., Wiekhorst, F., Steinhoff, U., Trahms, L., 2006, "Aggregation Behavior of Magnetic Nanoparticle Suspension Investigated by Magnetorelaxometry," *Journal of Physics: Condensed Matter*, **18**, 38.

Ekambara, K., Sanders, R., Nandakumar, K., Masliyah, J., 2009, "Hydrodynamic Simulation of Horizontal Slurry Pipeline Flow using ANSYS-CFX," *Industrial and Engineering Chemistry Research*, **48**, 17.

Erb, R., Sebba, D., Lazarides, A., Yellen, B., 2008, "Magnetic Field Induced Concentration Gradients in Magnetic Nanoparticle Suspensions: Theory and Experiment," *Journal of Applied Physics*, **103**, 06.

Ganguly, R., Sen, S., Puri, I., 2004, "Heat Transfer Augmentation using a Magnetic Fluid under the Influence of a Line Dipole," *Journal of Magnetism and Magnetic Materials*, **271**, 1.

Hajdu, A., Illes, E., Tombacz, E., Borbath, I., 2009, "Surface Charging, Polyanionic Coating and Colloid Stability of Magnetite Nanoparticles," *Colloids and Surfaces A: Physicochemical and Engineering Aspects*, **347**, 1.

Heris, S., Etemad, S., Esfahany, M., 2006, "Experimental Investigation of Oxide Nanofluids Laminar Flow Convective Heat Transfer," *International Communications in Heat and Mass Transfer*, **33**, 3.

Hetsroni, G., Mosyak, A., Pogrebnyak,, 2002, "Effect of coarse particles on the heat transfer in a particle-laden turbulent boundary layer**,"** Int. J. Multiph. Flow, **28,**12.

Incropera, F.P., DeWitt, D.P., Bergman, T.L., and Lavine, A.S., 2007, *Introduction to Heat Transfer*, J. Wiley & Sons.

Kaloni, P., Venkatasubramanian, S., 2008, "Flow of a Magnetic Fluid Between Eccentric Rotating Disk," *Journal of Magnetism and Magnetic Materials*, **320**, 3, pp.142-149.

Kobayashi, T., Tai, H., Kato, S., 2006, "Measurment Methods of Particle Concentration and Acoustic Properties in Suspension using a Focused Ultrasonic Impulse Radiated from a Plano-Concave Transducer," *Ultrasonics*, **44**, Supplement 1.

Lee, J., Flynn, R.D., Goodson, K.E., Eaton, J.K., 2007, "Convective Heat Transfer of Nanofluids (DI Water-Al2O3) in Microchannels," *Proceedings of 2007 ASME Thermal Engineering Summer Heat Transfer Conference*.

Mao, J., Aleksandrova, S., Molokov, S., 2008, "Joule Heating in Magnetohydrodynamic Flows in Channels with Thin Conducting Walls," *International Journal of Heat and Mass Transfer*, **51**, 17, pp. 4392-4399.

Murray, M.M., 2007, "Heat transfer enhancement using ferromagnetic particle laden fluid and oscillating magnetic fields," *Proceedings of the ASME/JSME Thermal Engineering Summer Heat Transfer Conference*, 2, pp 107-113.

Nasiruddin, M., Siddiqui,K., 2007, "Heat Transfer Augmentation in a Heat Exchanger Tube using a Baffle," *International Journal of Heat and Fluid Flow*, **28**, 2, pp 318-328.

Royon, L., Guiffant, G., 2008, "Forced Convection Heat Transfer with Slurry of Phase Change Material in Circular Ducts: A Phenomenological Approach," *Energy Conversion and Management*, **49**, 5, pp. 928-932.

Scherer, C., Neto, A., 2005, "Ferrofluids: Properties and Applications," *Brazilian Journal of Physics*, **35,** 3A.

Steinke, M.E., and Kandlikar, S.G., 2004, "Single-Phase Heat Transfer Enhancement Techniques in Microchannel and Minichannel Flows," *Proceedings of 2nd International Conference on Microchannels and Minichannels*, June 2004.

Vékás, L., 2007"Ferrofluids: Synthesis, Structure, Properties and Applications,"*New Magnetic Materials and Their Functions, European School of Magnetism*¸ September 2007.

Wang, L., Xiaohao, W., 2009, “Nanofluids: Synthesis, Heat Conduction and Extension,” *Journal of Heat Transfer*, **131**, 3.

Winterton, R.H., 1998, “Where Did The Dittus and Boelter Equation Come From?,” *International Journal of Heat and Mass Transfer*, **41**, 4, pp 809-810.

Xuan, Y., Roetzel, W., 2000, “Conceptions for Heat Transfer Correlation of Nanofluids,” *International Journal of Heat and Mass Transfer*, **43**, 19, pp 3701-3707.

Yang, H., Hong, T, Choi, S., 2005, “Study of the Enhanced Thermal Conductivity of Fe Nanofluids,” *Journal of Applied Science*, **97**.

Yoo, D.H., Hong, K.S., Yang, H., 2006, “Study of Thermal Conductivity of Nanofluids for the Application of Heat Transfer Fluids,” *Thermochimica Acta*, **455**, 1, pp. 66-69.

Yung, R., Rusu, S., Shoemaker, K., 2002, “Future Trend of Microprocessor Design,” *Proceedings of 28th European Solid-State Circuits Conference*.